

REPORT DOCUMENTATION PAGE			Form Approved OMB NO. 0704-0188		
<p>The public reporting burden for this collection of information is estimated to average 1 hour per response, including the time for reviewing instructions, searching existing data sources, gathering and maintaining the data needed, and completing and reviewing the collection of information. Send comments regarding this burden estimate or any other aspect of this collection of information, including suggestions for reducing this burden, to Washington Headquarters Services, Directorate for Information Operations and Reports, 1215 Jefferson Davis Highway, Suite 1204, Arlington VA, 22202-4302. Respondents should be aware that notwithstanding any other provision of law, no person shall be subject to any penalty for failing to comply with a collection of information if it does not display a currently valid OMB control number.</p> <p>PLEASE DO NOT RETURN YOUR FORM TO THE ABOVE ADDRESS.</p>					
1. REPORT DATE (DD-MM-YYYY) 27-09-2014		2. REPORT TYPE Final Report		3. DATES COVERED (From - To) 1-Jun-2009 - 31-May-2014	
4. TITLE AND SUBTITLE Final Report: New Principles for Interfacial Engineering and Superstabilization of Biphasic Systems by Using Particles with Engineered Structure and Properties			5a. CONTRACT NUMBER W911NF-09-1-0224		
			5b. GRANT NUMBER		
			5c. PROGRAM ELEMENT NUMBER 611102		
6. AUTHORS Orlin D. Velev, Stephanie Lam			5d. PROJECT NUMBER		
			5e. TASK NUMBER		
			5f. WORK UNIT NUMBER		
7. PERFORMING ORGANIZATION NAMES AND ADDRESSES North Carolina State University 2901 Sullivan Drive Suite 240, Campus Bx 7514 Raleigh, NC 27695 -7003			8. PERFORMING ORGANIZATION REPORT NUMBER		
9. SPONSORING/MONITORING AGENCY NAME(S) AND ADDRESS (ES) U.S. Army Research Office P.O. Box 12211 Research Triangle Park, NC 27709-2211			10. SPONSOR/MONITOR'S ACRONYM(S) ARO		
			11. SPONSOR/MONITOR'S REPORT NUMBER(S) 56041-CH.10		
12. DISTRIBUTION AVAILABILITY STATEMENT Approved for Public Release; Distribution Unlimited					
13. SUPPLEMENTARY NOTES The views, opinions and/or findings contained in this report are those of the author(s) and should not be construed as an official Department of the Army position, policy or decision, unless so designated by other documentation.					
14. ABSTRACT We have developed new types of particle stabilizers for Pickering foams and emulsions with extraordinary properties. The addition of magnetic particles into the superstabilizer particle made possible the formation of a unique new system – magnetically responsive foams, which can be destroyed and collected rapidly and on demand with the application of an external magnetic field. Quantitative models for magnetophoretic foam breakdown and rheology were developed. We also invented and characterized a new type of responsive foam based on thermoresponsive fatty acid tubes and carbon black particles. This system can be tuned to be uniquely multi-					
15. SUBJECT TERMS responsive materials, smart foams, foam stability, colloidal science, magnetic particles, detoxification					
16. SECURITY CLASSIFICATION OF:			17. LIMITATION OF ABSTRACT	18. NUMBER OF PAGES	19a. NAME OF RESPONSIBLE PERSON
a. REPORT	b. ABSTRACT	c. THIS PAGE			Orlin Velev
UU	UU	UU	UU		19b. TELEPHONE NUMBER 919-513-4318

Report Title

Final Report: New Principles for Interfacial Engineering and Superstabilization of Biphasic Systems by Using Particles with Engineered Structure and Properties

ABSTRACT

We have developed new types of particle stabilizers for Pickering foams and emulsions with extraordinary properties. The addition of magnetic particles into the superstabilizer particle made possible the formation of a unique new system – magnetically responsive foams, which can be destroyed and collected rapidly and on demand with the application of an external magnetic field. Quantitative models for magnetophoretic foam breakdown and rheology were developed. We also invented and characterized a new type of responsive foam based on thermoresponsive fatty acid tubes and carbon black particles. This system can be tuned to be uniquely multi-stimuli-responsive. We characterized how system composition affected foam response to UV light as a function of the amount of fatty acid, carbon black particles, and water content. We established the system properties necessary for efficient foam breakdown and demonstrated a unique magneto-photo-thermo responsive foam. Finally, we introduced novel particle superstabilizers made of lignin, a natural biomaterial. They can form the basis of a new class of by-design natural foam superstabilizers. All of these innovative systems can find application in chemical detoxification, spill collection and a variety of technologies. They have attracted significant interest from industrial collaborators.

Enter List of papers submitted or published that acknowledge ARO support from the start of the project to the date of this printing. List the papers, including journal references, in the following categories:

(a) Papers published in peer-reviewed journals (N/A for none)

<u>Received</u>	<u>Paper</u>
01/06/2010	1.00 Sejong Kim, Harry Barraza, Orlin D. Velev. Reprint of a peer-reviewed manuscript: "Intense and selective coloration of foams stabilized with functionalized particles" , Journal of Materials Chemistry, (10 2009): . doi:
08/02/2011	4.00 Vinayak Rastogi, Krassimir P. Velikov, Orlin D. Velev. Microfluidic characterization of sustained solute release from porous supraparticles, Physical Chemistry Chemical Physics, (12 2010): 0. doi: 10.1039/c0cp00119h
08/23/2012	5.00 Stephanie Lam, Elena Blanco, Stoyan K. Smoukov, Krassimir P. Velikov, Orlin D. Velev. Magnetically Responsive Pickering Foams, Journal of the American Chemical Society, (09 2011): 0. doi: 10.1021/ja205065w
09/19/2013	7.00 Elena Blanco, Stephanie Lam, Stoyan K. Smoukov, Krassimir P. Velikov, Saad A. Khan, Orlin D. Velev. Stability and Viscoelasticity of Magneto-Pickering Foams, Langmuir, (08 2013): 0. doi: 10.1021/la4014224
09/19/2013	6.00 Anne-Laure Fameau, Stephanie Lam, Orlin D. Velev. Multi-stimuli responsive foams combining particles and self-assembling fatty acids, Chemical Science, (08 2013): 3874. doi: 10.1039/c3sc51774h
09/19/2013	8.00 Harry Barraza, Sejong Kim, Orlin D. Velev. Intense and selective coloration of foams stabilized with functionalized particles, Journal of Materials Chemistry, (11 2009): 0. doi: 10.1039/b908054f
09/27/2014	9.00 Stephanie Lam, Krassimir P. Velikov, Orlin D. Velev. Pickering stabilization of foams and emulsions with particles of biological origin, Current Opinion in Colloid & Interface Science, (07 2014): 0. doi: 10.1016/j.cocis.2014.07.003
TOTAL:	7

Number of Papers published in peer-reviewed journals:

(b) Papers published in non-peer-reviewed journals (N/A for none)

<u>Received</u>	<u>Paper</u>
-----------------	--------------

TOTAL:

Number of Papers published in non peer-reviewed journals:

(c) Presentations

O. D. Velev, Scalable liquid-based manufacturing of functional nanomaterials. The First Annual Colloids & Surfaces Symposium at Virginia Tech, Blacksburg, VA April 2014.

Lam, S.; Blanco, E.; Smoukov, S. K.; Velikov, K. P.; Khan, S. A.; Fameau, A. L.; Velev, O. D. Novel Classes of Multi-Stimuli Responsive Pickering Foams, ACS Colloids 2014, Philadelphia (PA).

Lam, S.; Fameau, A. L.; Khan, S. A.; Velev, O. D. Engineering of Novel Classes of “Smart” Stimuli Responsive Foams, AIChE Annual Meeting 2013, San Francisco (CA).

Lam, S.; von Klitzing, R.; Velev, O. D. Biopolymer Particles for the Stabilization of Pickering Foams, IGRTG 1524 Meeting 2013, New Bern (NC).

(multiple presentations reported earlier listed below)

Lam, S.; Blanco, E.; Smoukov, S. K.; Velikov, K. P.; Khan, S. A.; Fameau, A. L.; Velev, O. D. Novel Classes of Stimuli Responsive Foams, 14th European Student Colloid Conference 2013, Potsdam-Golm (Germany).

Lam, S.; Blanco, E.; Fameau, A. L.; Smoukov, S. K.; Velikov, K. P.; Khan, S. A.; Velev, O. D. Functional Responsive Foams Stabilized with Particles of Engineered Structure and Shape, 245th ACS National Meeting and Exposition 2013, New Orleans (LA).

Lam, S.; Blanco, E.; Smoukov, S. K.; Velikov, K. P.; Khan, S. A.; Velev, O. D. Formulation and Characterization of a Novel Class of Magnetically Responsive Pickering Foam, ICR Meeting 2012, Lisbon (Portugal).

O. D. Velev, Particles 2013, Dayton, OH, August 2013. Scalable fabrication of functional polymeric nanomaterials by liquid confinement and shear (keynote).

S. Lam, E. Blanco, S. K. Smoukov, K. P. Velikov, O. D. Velev, 86th ACS Colloid and Surface Science Symposium, Baltimore MD, June 2012. Functional responsive foams stabilized with particles of engineered structure and properties

Lam, S.; Blanco, E.; Smoukov, S.K.; Velikov, K.P.; Khan, S.A.; Velev, O.D. ACS Spring 2012 National Meeting & Exposition, San Diego (CA). Formulation and Characterization of a Novel Class of Magnetically Responsive Pickering Foams.

Blanco, E.; Lam, S.; Smoukov, S.K.; Velikov, K.P.; Khan, S.A.; Velev, O.D. AIChE Annual Meeting 2011, Minneapolis (MN). Stability and viscoelasticity of responsive magneto?Pickering foams,

Lam, S.; Blanco, E.; Smoukov, S.K.; Velikov, K.P.; Velev, O.D. 2011 IGRTG 1524 Annual Meeting, New Bern (NC). Formulation and Characterization of a Novel Class of Magnetically Responsive Pickering Foams.

Orlin D. Velev, Particles 2011 conference, Berlin, July 2011. Keynote talk: Functional Magnetically Responsive Foams Stabilized with Particles of Engineered Structure and Properties.

S. Lam, A. Tibbits, O. D. Velev, 85th ACS Colloid and Surface Science Symposium, June 2011, Montreal, Canada. Synthesis and Characterization of Lignin Particles for Colloidal Stabilization.

E. Blanco, S. Lam, S. Smoukov, K. P. Velikov, O. D. Velev, 85th ACS Colloid and Surface Science Symposium, June 2011, Montreal, Canada. Magnetically Responsive Pickering Foams.

Orlin D. Velev, Department of Materials Science, ETH-Swiss Federal Institute of Technology, Zurich, Switzerland, November 2010. Invited talk: Foam Superstabilization and Functionalization by Particles with Engineered Structure and Properties.

Orlin D. Velev, EUFOAM 2010, Borovetz, Bulgaria, July 2010. Plenary Talk: Foam Superstabilization and Functionalization by Particles with Engineered Structure and Properties.

Orlin D. Velev, Sejong Kim, Qixin Zhong, Harry Barraza, AIChE Annual Conference, Nashville, TN, November 2009. Talk: Superstabilization and Functionalization of Foams and Emulsions by Particles with Engineered Structure and Properties.

Number of Presentations: 4.00

Non Peer-Reviewed Conference Proceeding publications (other than abstracts):

Received Paper

TOTAL:

Number of Non Peer-Reviewed Conference Proceeding publications (other than abstracts):

Peer-Reviewed Conference Proceeding publications (other than abstracts):

Received Paper

TOTAL:

Number of Peer-Reviewed Conference Proceeding publications (other than abstracts):

(d) Manuscripts

Received Paper

08/04/2011 3.00 Elena Blanco,, Stoyan Smoukov,, Krassimir P. Velikov,, Orlin D. Veleev, Stephanie Lam,, Magnetically Responsive Pickering Foams, (submitted) (08 2011)

TOTAL: 1

Number of Manuscripts:

Books

Received

Book

TOTAL:

Received

Book Chapter

TOTAL:

Patents Submitted

Patents Awarded

Awards

Orlin D. Velev - Springer 1st Colloid and Polymer Science Lecture Award 2014.

Stephanie Lam - 2014 NRC Postdoctoral Fellowship (National Research Council).

Stephanie Lam - 1st Place, Schoenborn Graduate Research Symposium Poster Prize, NC State, 2013.

(Previously reported awards)

Orlin D. Velev - Alumni Distinguished Undergraduate Professor (NC State University) 2013

Orlin D. Velev - NC ACS 2013 Distinguished Speaker Award (NC ACS Section) 2013

Orlin D. Velev - Innovator of the Year Award NC State University 2011.

Orlin D. Velev - Elected Fellow of the American Chemical Society, ACS, 2011.

Orlin D. Velev - Alumni Association Outstanding Research Award, NC State University 2011.

Orlin D. Velev - Alcoa Foundation Distinguished Engineering Research Award, NC State University, 2010.

Graduate Students

<u>NAME</u>	<u>PERCENT SUPPORTED</u>	Discipline
Stephanie Lam	1.00	
Tian Tian	0.25	
FTE Equivalent:	1.25	
Total Number:	2	

Names of Post Doctorates

<u>NAME</u>	<u>PERCENT SUPPORTED</u>
FTE Equivalent:	
Total Number:	

Names of Faculty Supported

<u>NAME</u>	<u>PERCENT SUPPORTED</u>	National Academy Member
Orlin D Velev	0.50	
FTE Equivalent:	0.50	
Total Number:	1	

Names of Under Graduate students supported

<u>NAME</u>	<u>PERCENT SUPPORTED</u>	Discipline
Taylor Thorton	0.00	Chemical Engineering
FTE Equivalent:	0.00	
Total Number:	1	

Student Metrics

This section only applies to graduating undergraduates supported by this agreement in this reporting period

The number of undergraduates funded by this agreement who graduated during this period: 1.00

The number of undergraduates funded by this agreement who graduated during this period with a degree in science, mathematics, engineering, or technology fields:..... 1.00

The number of undergraduates funded by your agreement who graduated during this period and will continue to pursue a graduate or Ph.D. degree in science, mathematics, engineering, or technology fields:..... 0.00

Number of graduating undergraduates who achieved a 3.5 GPA to 4.0 (4.0 max scale):..... 1.00

Number of graduating undergraduates funded by a DoD funded Center of Excellence grant for Education, Research and Engineering:..... 0.00

The number of undergraduates funded by your agreement who graduated during this period and intend to work for the Department of Defense 0.00

The number of undergraduates funded by your agreement who graduated during this period and will receive scholarships or fellowships for further studies in science, mathematics, engineering or technology fields:..... 0.00

Names of Personnel receiving masters degrees

<u>NAME</u>
Total Number:

Names of personnel receiving PhDs

<u>NAME</u> Stephanie Lam Tian Tian Total Number:	2
---	----------

Names of other research staff

<u>NAME</u>	<u>PERCENT SUPPORTED</u>
FTE Equivalent:	
Total Number:	

Sub Contractors (DD882)

Inventions (DD882)

Scientific Progress

(Detailed scientific report and ARO-type quad chart provided as attachments)

Technology Transfer

Stephanie Lam, Elena Blanco, Stoyan K. Smoukov, Krassimir P. Velikov, Orlin D. Velez, "Magnetically Responsive Pickering Foams" Invention disclosure, NCSU, 2012.

This research has resulted in significant interest and discussions with the following companies:

* Syngenta, Greensboro, NC

* Unilever, Port Sunlight, UK

* Unilever, Vlaardingen, The Netherlands

* P & G, Cincinnati, OH

The results of the work were of help to an NC State spin-off company, Xanofi.

The results of the work were of help to an NC State spin-off company, Benanova.

The project has allowed establishing research collaborations the the group of Prof. Regine von Klitzing, Technical University – Berlin and Dr. Elaine Hubal, Environmental Protection Agency (RTP).

New Principles for Interfacial Engineering and Superstabilization of Biphase Systems by Using Particles with Engineered Structure and Properties

Researchers

- **PI: Orlin D. Velev, NC State University**
- Stephanie Lam, Graduate Student, obtained PhD
- Elena Blanco-Castineiras, Visiting Postdoctoral Scholar
- Anne-Laure Fameau, Visiting Researcher

Deliverables:

- Synthesis of a variety of new types of particles through environmentally friendly processes
- Investigation of particle adsorption layers and films
- Investigation of foam and emulsion stabilization using synthesized particles

Selected recent publications:

Lam, S.; Velikov, K. P.; Velev, O. D. Pickering Stabilization of Foams and Emulsions with Particles of Biological Origin. *Curr. Opin. Colloid Interface Sci.* **2014**, DOI: 10.1016/j.cocis.2014.07.003.

Fameau, A. L.; Lam, S.; Velev, O. D. Multi-Stimuli Responsive Foams Combining Particles and Self-assembling Fatty Acids. *Chem. Sci.* **2013**, 4, 3874 – 3881.

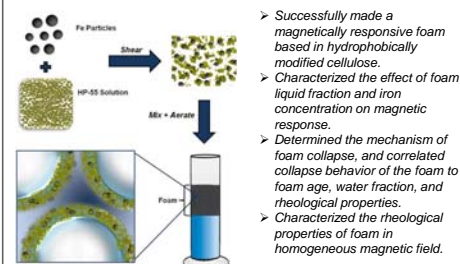
Blanco, E.; Lam, S.; Smoukov, S. K.; Velikov, K. P.; Khan, S. A.; Velev, O. D. Stability and Viscoelasticity of Magneto-Pickering Foams. *Langmuir* **2013**, 29, 10019–10027.

Lam, S.; Blanco, E.; Smoukov, S. K.; Velikov, K. P.; Velev, O. D. Magnetically Responsive Pickering Foams. *J. Am. Chem. Soc.* **2011**, 133, 13856–13859.

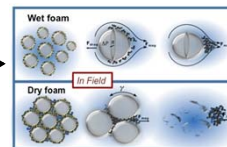
Biopolymer-based Foam with On-demand Destruction

Magneto-Pickering Foam Based on Cellulose Particles

Scheme: Fabrication Procedure



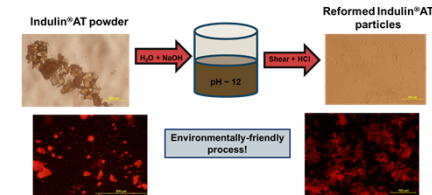
Proposed Mechanism



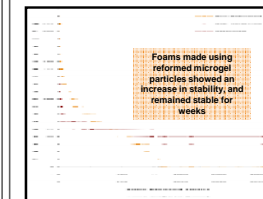
The results are interpreted within an adequate theoretical framework

Biopolymer Foams from Lignin Microgel Particles

Scheme: Fabrication Procedure



Result: Increased Foam Stability



- Reformed Kraft lignin into voluminous particle aggregates using a water based process.
- Studied properties of the particle dispersion such as zeta potential, effective volume, and morphology of particle aggregates.
- Characterized the ability of the reformed particles to stabilize foam.

Manuscript for dissemination of research results under preparation

Results



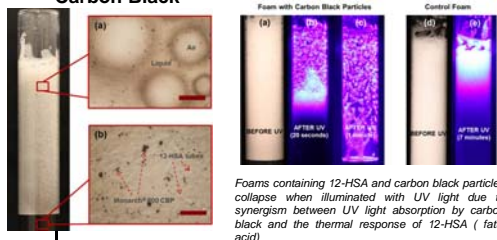
- Developed and characterized three novel responsive foam systems with special properties – see results panels on right

ARMY/DOD RELEVANCE

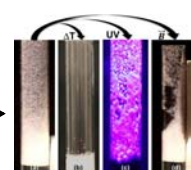
- The new responsive foams can be used in new efficient detoxification/cleanup procedures where toxic material is rapidly covered and detoxified by a foam head
- Can be used in new products for destruction of chemical agents in the field
- The unwanted foam/toxin residue can be collected rapidly
- Formulation of new Army field products with decreased environmental footprint

Multi-Stimuli Responsive Foams

Foam with 12-HSA and Carbon Black



Replace carbon black particles with iron particles



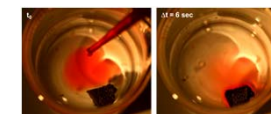
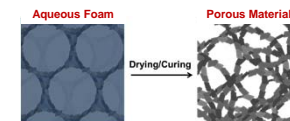
Multi-Stimuli Responsive Foam!

Results

- Invented a new foam which can be controllably collapsed using light.
- Characterized the effect of foam liquid content, fatty acid concentration and carbon black concentration on collapse properties.
- Fabricated a foam which can respond to light, magnetic field, as well as changes in temperature by replacing carbon black with iron particles.

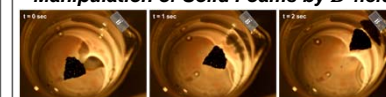
Solid Magnetic Foam

- Magnetically responsive foams stabilized using cellulose are made solid using lyophilization



Solid HP/Fe foam selectively absorbs oil (red-colored fluid in photo)

Manipulation of Solid Foams by B-field



After oil absorption, directional movement of HP/Fe foam on water surface can be manipulated using magnetic field

Results:

- (1) Evaluated the ability of solid HP/Fe foam to remove hydrophobic contaminants from aqueous systems.
- (2) Suggested other aqueous responsive foam systems for the generation of solid foams manipulatable by a gradient field.

Final Technical Report – ARO Project 56041CH

Orlin D. Velev, North Carolina State University

Abstract

We have developed new types of particle stabilizers for Pickering foams and emulsions with extraordinary properties. We use particles made of hydrophobically modified cellulose that result in the formation of super-stable foams. First we showed how the inclusion of dyes in these particles allows making of colored foams, which can find a variety of applications. The addition of magnetic particles into the superstabilizer particles made possible the formation of a unique new system – magnetically responsive foams. These novel “magneto-Pickering” foams exhibit excellent stability in the absence of a gradient magnetic field, but can be destroyed rapidly and on demand with the application of a threshold field. We correlated the collapse behavior of the foams to the liquid fraction as well as the concentration of magnetic particles in the lamellae. We also characterized the rheological stability of the foam and developed quantitative models for magnetophoretic foam breakdown. In a collaborative work with TU-Berlin, we elucidated the mechanisms by which the particles stabilize foams by examining foam films containing these particles. More recently, we also demonstrated the generation of a solid, magnetically responsive, porous material from the aqueous foam system. More recently, we introduced a novel multi-responsive foam system based on thermoresponsive fatty acid tubes and carbon black particles. Like the magneto-responsive foams, this system is also stimuli-responsive, but is responsive to light stimulus rather than magnetic stimulus. We studied how system composition affected foam response to UV light by varying the amount of fatty acid, carbon black particles, as well as water. We determined system properties necessary for efficient foam breakdown and demonstrated that such foams can also be collapsed using solar illumination. Lastly, we developed new particle superstabilizers made of lignin, a natural biomaterial. We have demonstrated how the stabilization efficiency of lignin can be increased dramatically by water-based reforming. We characterize the surface charge and solubility of the reformed and non-reformed particles, and observe the nature of the particle aggregates of the reformed lignin particles. On this basis, we are developing a new class of “designed” natural foam superstabilizers. All of these new systems can find application in chemical detoxification, spill collection and a variety of technologies. They have attracted significant interest from industrial collaborators.

Motivation and background

It has been known since the beginning of the 20th century that particles with the appropriate wettability can impart greater stability to foams and emulsions than molecular surfactant stabilizers.^{1, 2} However, research in the area of Pickering foams and emulsions has mostly been focused on studying the effect that the properties of inorganic particles (wettability, concentration, size, and shape) have on the stability of these systems; little research has been performed in the development and characterization of particle stabilizers made from biodegradable materials.³⁻⁵ In the results of the ARO-supported research presented here, we evaluated the ability of naturally derived materials to stabilize foams and emulsions. Wege et al. had previously demonstrated that hydrophobically modified cellulose, HP-55, can be used to generate superstable foams.⁶ Our group then demonstrated that functionality (such as color) could be imparted on the HP-55 foam matrix through the use of a hydrophobic dye.⁷ Building on that concept, we developed a class of magnetically responsive foams by suspending carbonyl iron particles in the HP-55 matrix. These responsive systems can be defoamed on demand with the application of a magnetic field. We also observed a difference in the collapse behavior of fresher (5 hour, 1 day) foams versus that of older foams (3+ days). This led us to formulate a mechanism for the collapse behavior of the foam. Here, we report data that we have acquired by characterizing the difference in the properties of the fresh and old foams that contribute to their breakdown, and also refine our hypothesis pertaining to the mechanism behind the destruction of our foams.

In a collaborative project with scientists from Technical University in Berlin, we examined how the hydrophobically modified cellulose particles, which impart long-term stability onto the colored and magnetic foam systems, stabilize these biphasic dispersions. Cellulose, a linear polysaccharide which consists of β (1,4)-linked glucopyranose units, exists as a structuring agent in the walls of plant cells as well as some eukaryotes.^{8, 9} It is the most abundant polysaccharide found in nature and accounts for $\sim 1.5 \times 10^{12}$ tons of annual biomass production.¹⁰ As a result of its biodegradability, biocompatibility, and sustainability as a raw material, there has been much focus on the use of cellulosic materials for various applications ranging from lightweight products to pharmaceuticals and biomedical applications.^{11, 12} One type of cellulose which has been widely examined for food and medical applications is modified cellulose. It is approved for utilization in foods and pharmaceuticals as coatings and encapsulants, and has also been found to be useful in highly efficient foam and emulsion stabilizers.¹³⁻¹⁵ In this part of the project, we examined the mechanism of foam stabilization by micron-sized particles from hydroxypropyl methylcellulose phthalate (HPMCP) by comparing observations of foam films stabilized by HPMCP to bulk foams stabilized by the same cellulose. The particles appeared deformable when compressed in the foam lamella, and exhibited co-adsorption with soluble HPMCP molecules at the air-liquid interface. HPMCP was studied since it had previously been shown to have the capability of generating superstable foams with particle formation in situ during the foaming process.¹⁴ In addition, it more recently served as a basis for the design of functional foams, such as colored foam and magnetically responsive foam.¹⁶⁻¹⁸

A biologically derived molecule, 12-hydroxystearic acid (12-HSA), was recently reported to generate foams which are ultrastable. 12-HSA has been shown to self-assemble into tube-like structures, which jam in the plateau borders of foam, acting as a barrier to liquid drainage and bubble coarsening. Fameau et al. demonstrated that foams stabilized using tubular assemblies from this fatty acid remained stable until exposed to a temperature higher than $T_{\text{transition}}$ - the temperature at which the fatty acid assemblies in the foam change from tube-like structures to micelles.¹⁹ 12-HSA is produced by the hydrogenation of a sustainable material - ricinoleic acid from castor plants and is an inexpensive molecular surfactant available in large quantities. In the work presented here, we show how foam responsive to UV irradiation can be produced by combining 12-HSA with carbon black. To gain insight into the mechanisms responsible for the light-induced destabilization of this system, we varied fatty acid concentration, carbon black particle concentration, as well as the initial water fraction. To generalize our approach, we used other particles known to be absorbers of light radiation, such as metallic particles, and explored foam response to both light and magnetic fields.

Another biomaterial that we have been studying for the stabilization of foams and emulsions is lignin. In a previous report, we mentioned finding a grade of Kraft lignin we received from MeadWestvaco to dissolve in aqueous media at high pH. We also showed that we were able to stabilize foams using this material. In this report, we summarize the process used to make the particles and the foam; the characteristics (surface charge, morphology, effective volume) of the reformed particles compared to that of the original powder; as well as the ability of these particles to stabilize foams.

Technical Results

Foam Stabilization by Hydrophobically Modified Cellulose. In a collaborative project with scientists from Technical University in Berlin, we elucidated the mechanism of foam stabilization by particles from hydrophobically modified cellulose by examining the morphology and stability of foam films stabilized by hydrophobically-modified cellulose (HP-55 or HPMCP) using a Thin Film Pressure Balance (TFPB) apparatus.

Cellulose particles used in foam and foam film stabilization were generated by precipitating HP-55 polymer out of solution by lowering the pH of the polymer solution under shear. The generated particles are polydisperse and range from 7.5 μm -10.5 μm in diameter with an aspect ratio varying from 2-2.5. They also exist as aggregates in suspension (**Figure 1**). This is most likely due to the low ζ -potential of the particles at the test pH (~ 4) as well as their large size. ζ -potential measurements were performed using smaller (model) HPMCP particles as described above and was determined to be ~ -21 mV at the pH at which foams were generated in this study (**Figure 2**).

Suspensions of varying HP-55 concentrations were foamed using a high shear mixer (Oster Model 4242). The foam volume as well as volume of liquid drained from the air-rich phase was

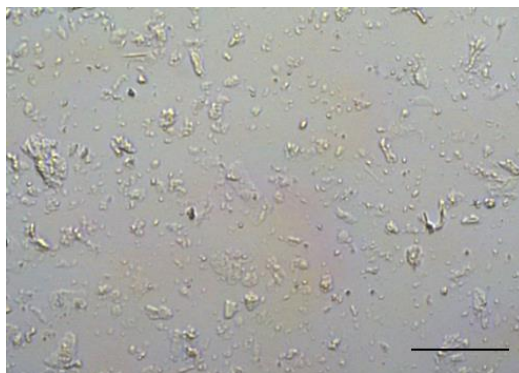


Figure 1. Micrograph showing HP-55 particle aggregates. Scale bar = 100 μm .

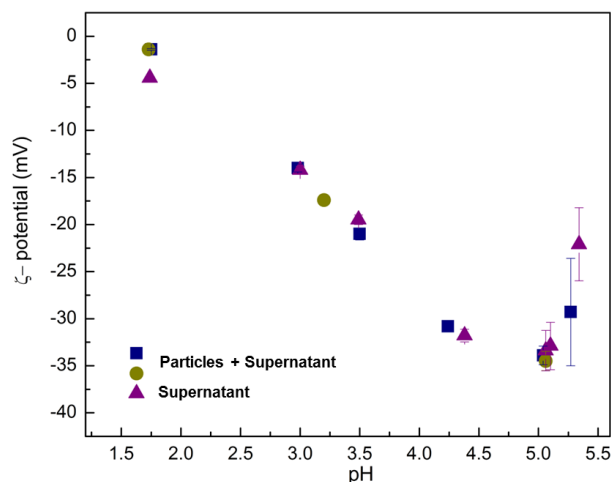


Figure 2. ζ -potential of HP-55 suspension (particles + supernatant) (■, ●) and supernatant (▲). ζ -potential increases with an increase in pH and begins to decrease near the pH at which HP-55 dissolves back into solution.

monitored overtime. As expected, foams containing higher concentrations of HP-55 not only maintained a larger head volume over longer periods of time, but also had better foamability. This is because when HP-55 concentration is increased, a larger quantity of dispersed HP-55 molecules are available to stabilize the air-liquid interface created during the foaming process. In addition, with increasing HP-55 concentration, more precipitated particles would also be available to sterically stabilize the disperse (air) phase. As in most particle stabilized systems, HP-55 particles will form a shell around the bubbles in the foam to prevent coalescence and hinder coarsening. In addition, they will also jam in the foam lamella and plateau borders to slow the drainage of liquid from the foam head (**Figure 3**). After bubbles extracted from foam stabilized by 1% HP-55 were air dried for 5

hours, they remained intact whereas bubbles from foam containing only 0.2% HP-55 did not demonstrate any stability against drying (**Figure 4**). This shows that a critical concentration of particles is necessary to stabilize the air-liquid interface in the foam system.

If the foam volume or liquid volume decay times are extracted from the experimental data shown in **Figure 3** and plotted as a function of HP-55 concentration, it can be noted that there is a critical break which occurs between $[\text{HP-55}] = 0.63\%$ and $[\text{HP-55}] = 0.75\%$ (**Figure 5**). Within this range of concentrations, the foam makes a transition from low to high stability. From this, it can be deduced that the minimum volume fraction of particles necessary to stabilize the air-liquid interface in this system is between 10-12 vol% of particles in the pre-foamed liquid dispersion.

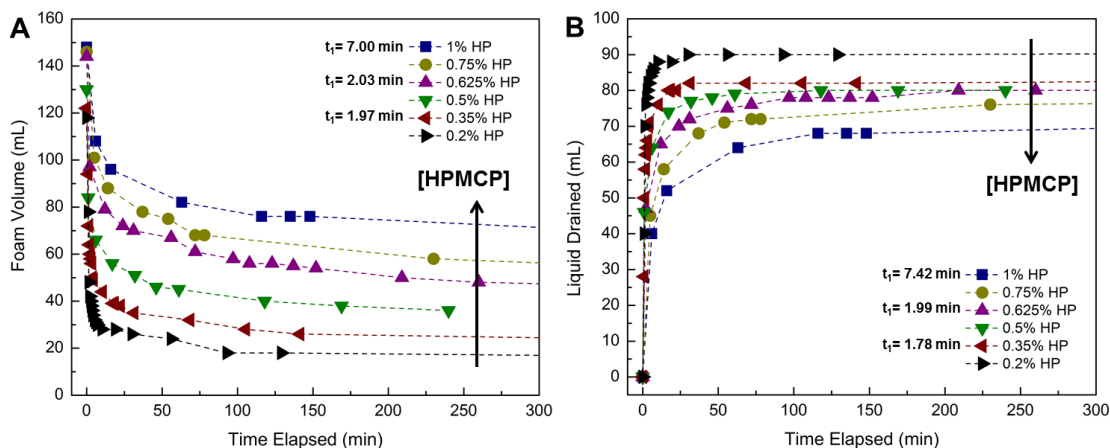


Figure 3. (a) Foam volume vs. time for foams containing varying concentrations of HP-55. (b) Liquid volume drained from foam vs. time for foams containing varying concentrations of HP-55.

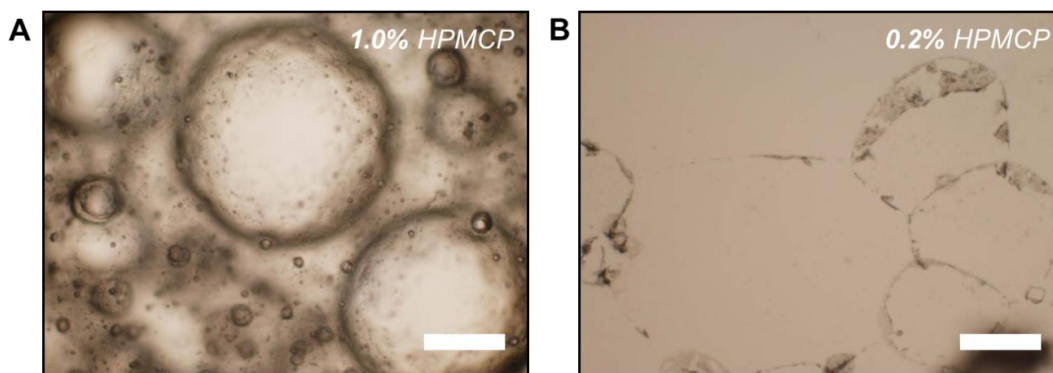


Figure 4. (a) Bubbles from 1 w/v% HP-55 foam after air drying for 5 hours. (d) Bubbles from 0.2 w/v% HPMCP foam after air drying for 5 hours.

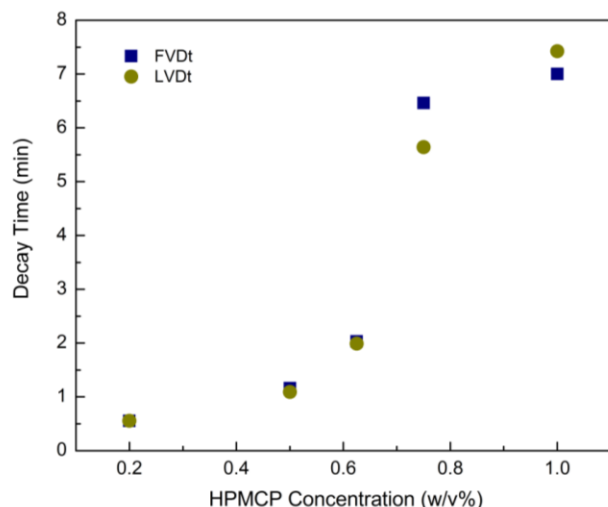


Figure 5. Foam volume decay time (FVDt) and liquid volume decay time (LVDt) as a function of cellulose concentration.

To better understand the mechanism by which HP-55 stabilizes air-liquid dispersions, foam films containing the modified cellulose were observed in a TFPB. When a liquid meniscus formed by a 1% HP-55 dispersion was thinned in the apparatus, we observed the formation of gels from the compression of HP-55 particles in the hole of the porous disc (**Figure 6**). Thus, at high cellulose concentrations (which were used in our previous work) foams are sterically stabilized by particle gel networks, which form in the lamella of the foam subsequent to gravitational liquid drainage.¹⁶⁻¹⁸ Particle bridging would result in a higher effective viscosity in the continuous phase as well as the retardation of foam aging mechanisms - namely liquid drainage from the foam and interbubble gas diffusion.²⁰ For subsequent experiments, particle dispersions were diluted to 0.75%, 0.63%, 0.5%, 0.35%, and 0.2% HPMCP, and the morphologies of foam films formed by

these dispersions observed. The statistics of film vs. gel formation in the P2 frit are summarized in **Figure 7**. As seen in this figure, the likelihood of gel formation decreases with decreasing HP-55 concentration, exhibiting a critical transition between majority instances of gel formation and majority instances of film formation between HPMCP concentrations of 0.75% and 0.63%. These results correlate well with the transition observed in the decay times extracted from foaming experiments presented in the previous section (**Figure 5**). This implies that the concentration of particles in the system, which corresponds to varying degrees of interface coverage by particles in a bulk foam, can be well associated with the different types of film morphologies observed in the TFPB.

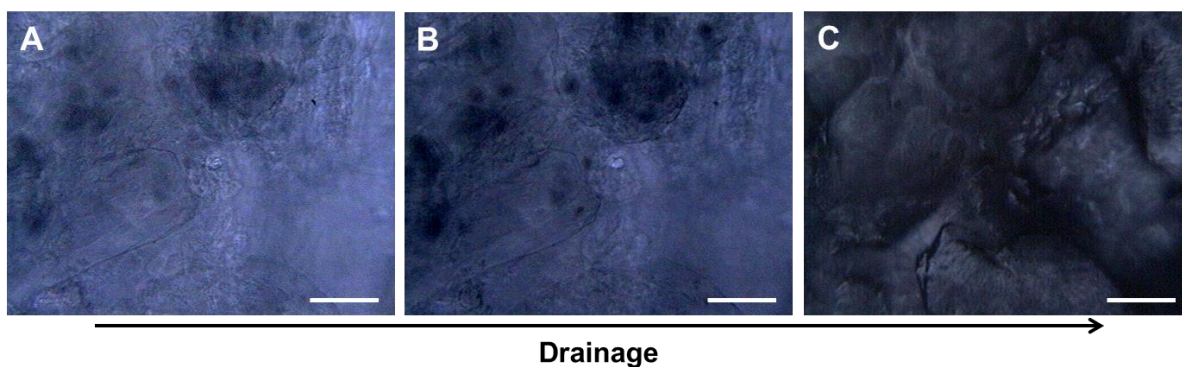


Figure 6. Micrographs following the thinning of gel-film stabilized by 1% w/v HP-55as observed in a TFPB. (a) Liquid meniscus containing large HP-55 aggregates prior to liquid drainage from capillary cell; (b) film during drainage; and (c) gel-film resulting from liquid drainage. Scale bar = 100 μm .

At non-gelling concentrations of HP-55, we observed the formation of nonhomogeneous thin films (**Figure 8**). As seen in these micrographs, thin films formed from lower concentration dispersions of HPMCP contain bright white spots inside a gray film. This shows that small HP-55 particles and (larger) particle aggregates can co-adsorb at the air-liquid interface along with dispersed HP-55 polymer, although it is unclear if this is the actual mechanism. Another possibility is that particles are trapped by the 2D polymer-gel network formed by dispersed HP-55 molecules.²¹⁻²³ It can be postulated that during the formation of cellulose foams, smaller particles and dispersed HP-55 polymer most likely diffuse first to the air-liquid interface with larger HP-55 particles and particle-aggregates forming a shell around the bubbles in a secondary adsorption step. As the concentration of HP-55 is increased in the test suspension, the number of particles trapped in the foam film also increases.

As the concentration of particles in the test suspension was increased, a higher number of large HP-55 particles was observed in the foam film (**Figure 8**). Further increase in HP-55 particle concentration resulted in the compression of the particles in the meniscus to form a solid gel upon liquid drainage from the porous frit. When the instances of film formation and gel formation were characterized as a function of HP-55 concentration in the test suspension, a transition between majority film formation and majority gel formation in the TFPB was observed between 0.63 w/v% and 0.75 w/v% HP-55. Since these data are commensurate with a sharp transition in the liquid drainage decay time which was extracted from foaming experiments, it can be concluded that HPMCP foams become superstable at particle concentrations where there is a high instance of particle gel formation in the foam film (of the bulk foam system) following liquid drainage. Thus, although dissolved HPMCP molecules can diffuse to the air-liquid interface more quickly and can form 2D-gels in thin liquid films, the presence of a certain threshold concentration of particles is ultimately necessary for a jump increase in foam and foam film stability (**Figure 9**).

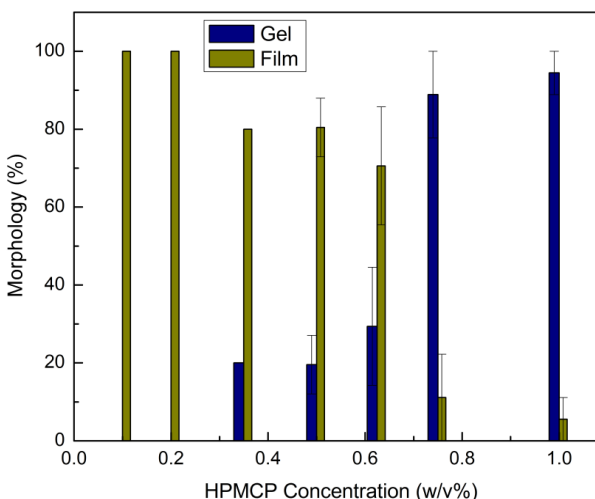


Figure 7. Statistics of gel vs. film formation for HP-55 dispersions at different concentrations. Percentages were calculated from ten films formed per sample with data for each concentration averaged over three different samples.

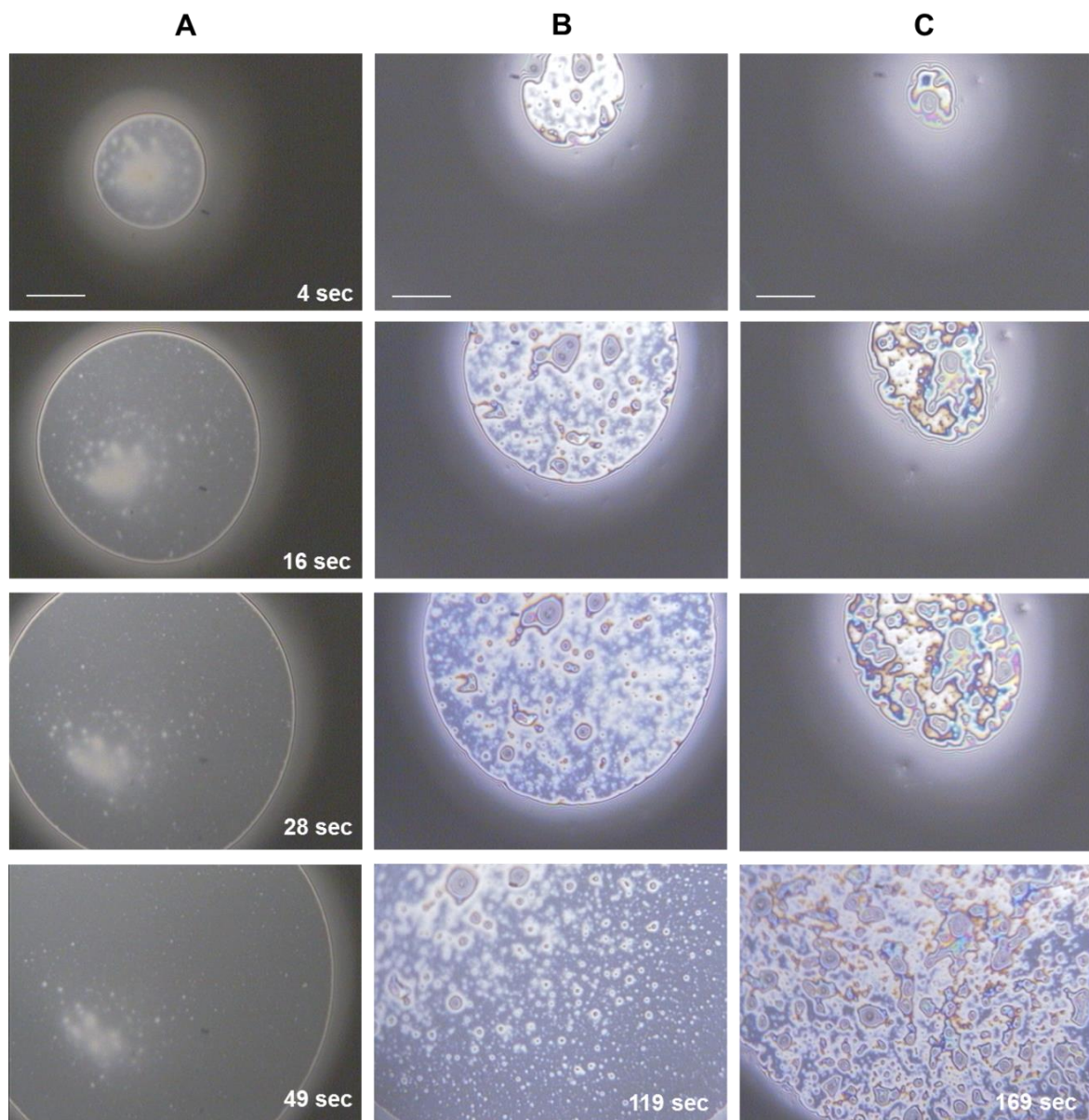


Figure 8. Micrographs showing film morphology as a function of HP-55 concentration. (Column A) 0.2 w/v% HP-55 suspension; (Column B) 0.35 w/v% HP-55 suspension; (Column C) 0.63 w/v% HP-55 suspension. The times shown represent time elapsed from initial film formation. Scale bar = 100 μm.

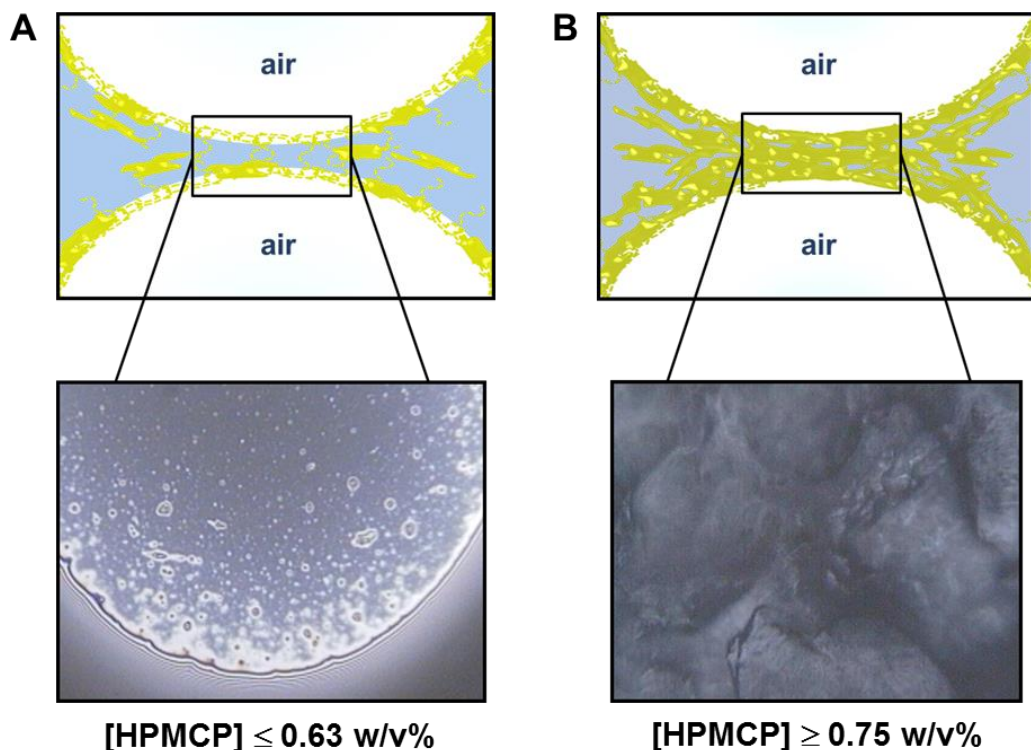


Figure 9. (a) Schematic of foam system with adsorbed HPMCP and micrograph of foam film stabilized by hydrophobized cellulose at concentrations below the transition threshold. Foams at these concentrations have short decay times as a result of insufficient interface coverage by particles. (b) Schematic of foam system with adsorbed HPMCP and micrograph of foam film stabilized by HPMCP at concentrations above the transition point. Sufficient interface coverage by particles results in steric stabilization of cellulose foams by the formation of a particle-gel network.

Future Perspectives. While examining the mechanism of HP-55 foam and foam film stabilization, it was noticed that in the system stabilized by modified cellulose particles, there also exists a molecularly dispersed species of HP-55 polymer in solution. This molecular species most likely helps to lower the tension at the air-liquid interface and can also impact the adsorption of HP-55 particles at the air-liquid interface in foam systems. Thus, future work will involve studies to examine the role of the dispersed polymeric species of HP-55 on the adsorption of HP-55 particles at the air-liquid interface and on foam and foam stability. A manuscript for the work presented above is currently in preparation. In the realm of foams stabilized by particles from naturally derived materials, we published a review article this year in *Current Opinion in Colloid and Interface Science*.²⁴

Magneto-Pickering Foams. In this project pertaining to the engineering of stimuli-responsive foams which are stable until collapsed using an external magnetic field, we elucidate the change in foam properties as a function of age, and correlate these changes to the destruction pattern of the foams. The time evolution of the water fraction in the magnetic foam system will be reported first since it serves as a basis for the explanation of the other properties that are measured in this work. We quantified the water fraction in our foams as a function of age (**Figure 10**) and demonstrated that our foams (2.7 wt% Fe) start with ~50% water and that after a week, still contain ~25% water. The standard classification used for foam water content, ϵ , is as follows: $\epsilon > 0.35$ (bubbly liquid); $\epsilon \sim 0.35$ (wet foam); $\epsilon < 0.01$ (dry foam).²⁵ This means that the liquid retention capability of the foam system studied here is much higher than that of conventional foam systems. We also compared the drainage behavior of our foam to surfactant foams

using a common drainage model which expresses water fraction as a function of time: $\varepsilon \sim t^{-\beta}$.²⁶ For surfactant foams, the value of β is usually between 2/3 and 1. For our system, the value of β_{\max} is 1/6, which tells us that our foams drain much slower than conventional foams.

Rheological properties of the foam such as the viscous and elastic moduli, G'' and G' respectively, were measured at different points during the aging process of the foam to determine the effect of aging on the viscoelastic properties of the foam. The experiments were performed using an AR2000 rheometer from TA instruments. In these experiments, G' and G'' were measured as a function of stress as well as angular frequency. We found that from a rheological standpoint, since $G' > G''$ for all the samples tested, our foams can be considered to be gel-like materials (**Figure 11a**). We also found from these measurements that as the foams age, the elastic modulus of the foam increases while the viscous modulus of the foam decreases (**Figs. 11a and 11b**). These data confirm the general model for age-dependent foam breakdown because as the foam ages, the films between the bubbles thin as a result of the drainage of water from the foam. This causes the bubbles and particles in the foam to pack closer together, causing drier foams to have a more elastic response when an oscillatory stress is applied. This effect is clearly outlined in **Fig. 11b**, which shows the decay of G''/G' overtime. G''/G' is a rheological parameter also known as $\tan\delta$, which is a measure of material damping.

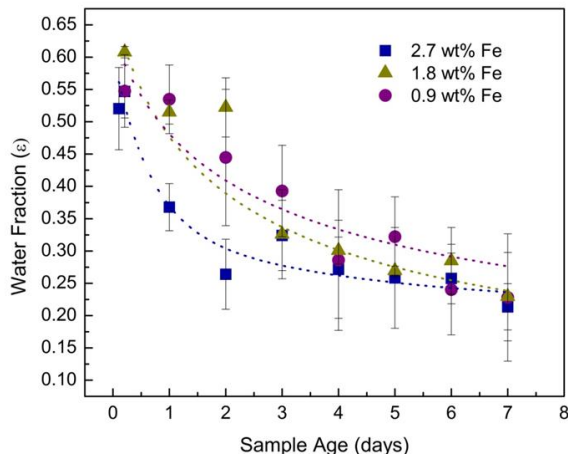


Figure 10. Foam water fraction as a function of time at different carbonyl iron concentrations. All samples make a transition from “wet” to “dry” foams.

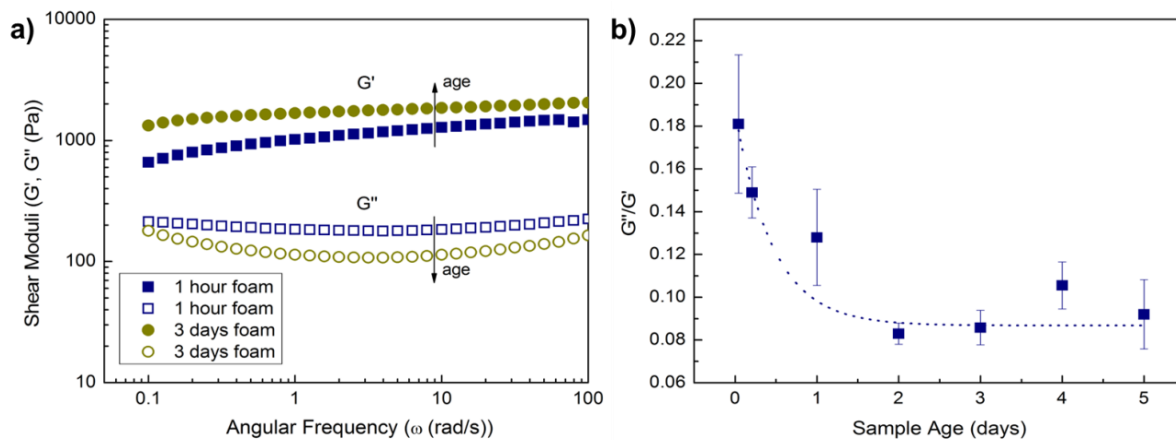


Figure 11. (a) Plot of G' and G'' as a function of angular frequency. The elastic modulus of the foam, G' , increases as the foam gets older while the viscous modulus of the foam, G'' , decreases with age. The shape of the curves, and the fact that $G' > G''$ are characteristic of a gel-like material. (b) Plot of G''/G' as a function of sample age. This plot shows that as the foam ages, elastic effects begin to dominate viscous effects.

The magnetization behavior of a fresh and one day old foam were measured using a SQUID to determine if there was a difference in the magnetic susceptibility of the two systems. The magnetization curves demonstrate that the one day old foam has a higher magnetization saturation value than the fresh foam (**Figure 12**). Using this data, we calculated the magnetic susceptibility, χ , of the two systems to be: $\chi_{\text{fresh}} = 0.0005 \text{ emu/gOe}$ and $\chi_{\text{old}} = 0.0022 \text{ emu/gOe}$. From this we can conclude that as the foam ages, the magnetic susceptibility per mass of foam increases. This effect is most likely the product of the drainage of water from the foam, which results in thinner films and an increase in the concentration of the magnetic particles per volume of foam remaining. Taking the magnetization data into account with the rheological and water fraction data, we can further refine and quantify the mechanism for foam destruction in the presence of a field.

Previously, we had proposed the hypothesis that fresher foams are more resistant to destruction by a magnetic field since its higher water content and thicker films allowed for the movement of loose iron particles around the bubbles. Drier foams, having lower water content and thinner films, provide no room for the rearrangement of loose particles and bubbles in a magnetic field. This results in the rapid destruction of older foams with respect to fresher foams. The data presented here supports part of this original hypothesis, and also offers a more complete explanation behind the different mechanisms of foam destruction in fresh and old foams. Fresh or younger foams have higher liquid content and thicker films. This does allow room for the rearrangement of loose particles when the system is exposed to a magnetic field.

The newly-formed foam systems are also less susceptible to a magnetic field as a result of the dispersion of iron particles in the system over a larger volume. Thus, when the foam is exposed to a magnetic field, the attractive force between the particles and the magnet is not high enough to rapidly destroy the foam. Optical microscope videos of the response of wet foam to a magnetic field show the presence of thick films; when a magnetic field is applied, the system travels as a whole toward the source of the field. The process of defoaming does not occur until the whole foam body has shifted toward the field. Drier or older foams have a lower liquid content and include thinner films, which allots little room for the loose iron particles to rearrange in a magnetic field. These foams also have a higher magnetic susceptibility because as water drains from the foam, the volume of the foam body shrinks resulting in an increase in the number of carbonyl iron particles per unit volume of foam. Thus, when these foams are exposed to a magnetic field, not only is the force of attraction between the magnetic particles and the magnet higher, but because the contents of the foam are more tightly packed, the particles induce tension on the films between the bubbles when travelling toward the magnet. This causes the films to break down, resulting in the rapid destabilization of the foam through bubble popping as well as bubble coalescence. The difference between these two scenarios is illustrated in **Figure 13**.

Additionally, we have derived two expressions to estimate the number of particles necessary to induce foam collapse in each of the scenarios. This was done to check whether the proposed mechanisms corroborated well with the components in the system. The minimum number of particles needed to collapse the foam in each scenario was evaluated as follows:

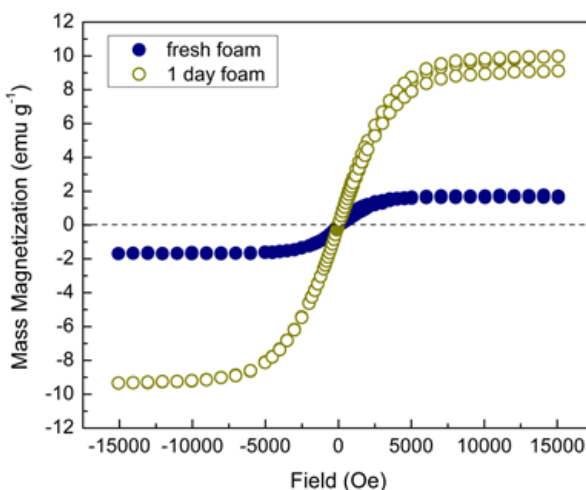


Figure 12. Magnetization curves for magneto-Pickering foams. These curves represent the mass magnetization as a function of applied magnetic field for fresh and 1-day old foams at 300 K and 2.7 wt% Fe.

$$N_p^{wet} \approx \frac{\Delta P \cdot \pi R_{bubble}^2}{F_{mag}} \quad (1)$$

$$N_p^{dry} \approx \frac{\gamma \cdot l_{stretch}}{F_{mag}} \quad (2)$$

In these expressions, F_{mag} is the magnetic force that the field exerts on one iron particle, N_p is number of particles, ΔP is the Laplace pressure inside an air bubble, R is the radius of the bubble, γ is the energy at the air-water interface, and $l_{stretch}$ is the length over which the particles act to stretch the bubble. For the fresh foam system, we evaluate the force that leads to the expulsion of one air bubble from the foam matrix. The pressure inside a bubble of radius R exceeds that outside it by the Laplace pressure ($\Delta P = 2\gamma/R$). To squeeze a bubble out of the foam matrix, a force must be exerted to overcome the Laplace pressure distributed over the cross-sectional area of the bubble (πR^2). In this case, the force that is exerted in opposition to the Laplace pressure is the force of attraction between the CI particles around the bubble and the applied magnetic field ($N_p^{wet} \vec{F}_{mag}$). In Eqn. 1, we have equated the Laplace pressure of one air bubble to the total force of attraction between the CI particles around the bubble to the magnetic field. This equation can be used to estimate the number of CI particles necessary to induce collapse by air expulsion from a fresh foam sample. As the foam ages, magnetic and HP particles are compressed and immobilized in the less fluid films as water drains out by gravity. The particles in the thin gel-like films

lose their mobility and exert collective stresses on the film when magnetized. In this model, the destruction of the dry foam is based on the rupture of thin films between adjacent bubbles. In Eqn. 2, we have equated the force needed to rupture a thin film ($\gamma l_{stretch}$) to the total force exerted on the film by the attraction between CI and the magnetic field ($N_p^{dry} F_{mag}$). In this model, the magnetic pull of the particles is opposed by the tension (γ) at the bubble surfaces.

We determined the minimum number of particles necessary to induce foam collapse in the case of wet and dry foams using the above derived expressions, and compared the values for the estimated number of particles needed to induce collapse to the actual number of particles in the foam head. The number of magnetic particles loaded into a foam can be approximated to be 2×10^{10} (considering a concentration of 2.7 wt % Fe). According to the expression above, approximately 4000 iron particles are needed to squeeze one bubble out of the wet foam matrix; and in the case of drier foams, approximately 600 iron particles are required to rupture a film. These values are consistent with the number of CI particles in the foam, validate our

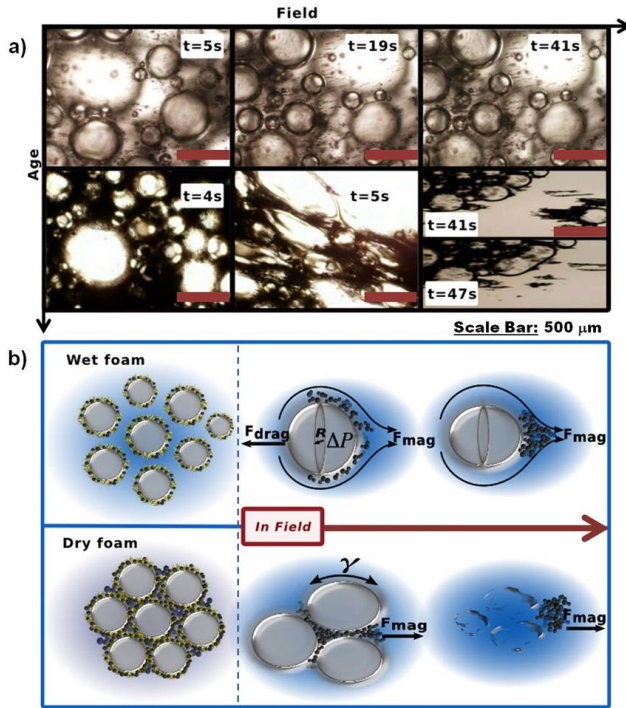


Figure 13. (a) Snapshots of microscopic collapse process for wet foam (top row) and dry foam (bottom row). (b) Mechanism of foam collapse as a function of age. Mechanism of collapse for wet foam - bubble ejection from particle matrix by magnetic field (top row). Mechanism of collapse for dry foam - film rupture via stretching by magnetic field (bottom row).

proposed collapse mechanisms, and give us a semi-quantitative estimate pertaining to the magnitude of the forces necessary to induce foam collapse. They also explain the drastic increase in the foam responsiveness and rate of destruction with time, as the number of particles in the aged system becomes nearly an order of magnitude larger than the one needed to induce foam destruction.

The effect of age on the magnetic properties of the foam was also exemplified in magnetorheology experiments performed for the HP/Fe system. Results from dynamic oscillatory experiments are presented below. From **Figure 14**, it can be seen that for a fresh foam sample the elastic modulus increases with an increase in the strength of the applied field. This effect results from the chaining of the carbonyl iron particles in the foam. As the strength of the applied magnetic field is increased, the strength of the particle chains resisting deformation also increases, resulting in improved rheological properties (increase in G'). The effect of the applied (homogeneous) magnetic field on the mechanical properties of the magnetic foams is similar to that typically observed for magnetorheological (MR) fluids.²⁷ In MR fluids, both the complex modulus and yield stress have been observed to be enhanced by the application of a magnetic field to induce an attractive force between the magnetically responsive particles in the sample. The strength of attraction between magnetic particles has been shown to increase with increasing field strength.²⁷⁻²⁹

By extracting the linear elastic modulus (G'_{lin}) and the yield stress (τ_y) from stress sweep curves like those presented in **Figure 14**, the relationship between G'_{lin} and τ_y and the strength of the applied field can be obtained (**Figure 15**). As seen in **Figure 15**, both G'_{lin} and τ_y increase with the strength of the applied field. As mentioned, the improved mechanical properties measured for the foam with increasing field strength results from an increase in the attractive force between magnetic particles in stronger magnetic fields. Another relationship which can be observed is that between the mechanical properties of the samples tested and the age of the samples. As shown in **Figure 15**, as the age of the sample increases, the linear modulus and yield stress also increase; this data agrees well with the dynamic oscillatory data presented above for magnetic foams tested using the AR2000 rheometer. The plots for G'_{lin} and τ_y as a function of sample age show a transition after ~ 1 day of aging, which was previously observed for the foam in the absence of a magnetic field (**Figures 10 and 11**). The age dependent rheological properties of the foam both in the absence and presence of a magnetic field most likely result from a change in foam microstructure with liquid drainage during the aging process. Additionally, the results in **Figure 15** also show aged foam samples to exhibit a stronger response to an increase in magnetic field strength. This result correlates well with our observations for foam collapse as well as with the data obtained from SQUID magnetometry.

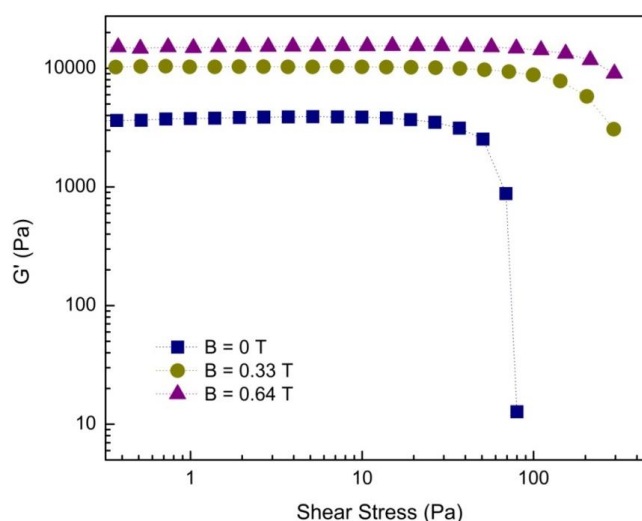


Figure 14. Storage modulus (G') as a function of shear stress for fresh foam samples tested under different magnetic field strengths. As the strength of the applied field is increased, G' also increases.

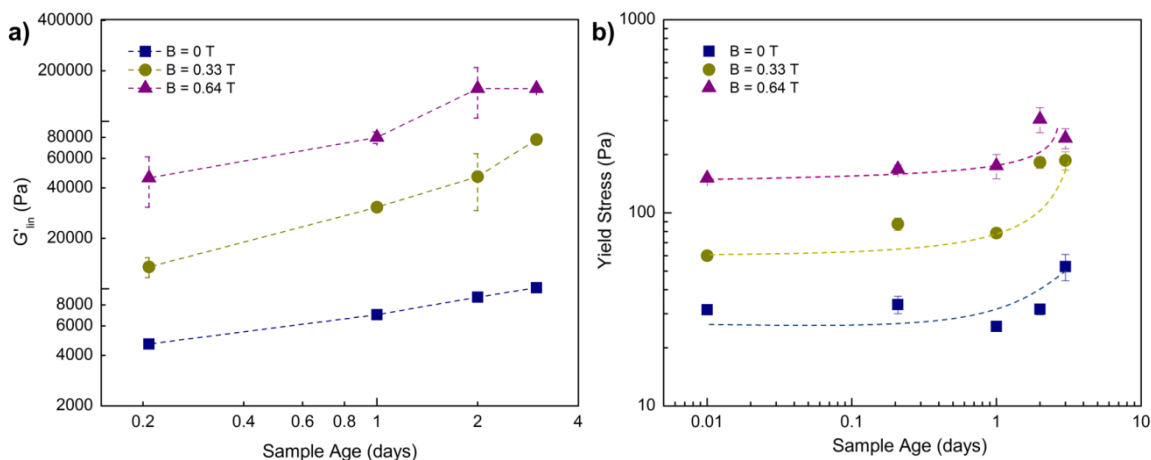


Figure 15. (a) Linear elastic modulus for HP/Fe foam samples as a function of sample age for foams tested when the strength of the applied field is: 0 T (blue), 0.33 T (yellow), and 0.64 T (purple). (b) Foam yield stress as a function of sample age for foams tested under different magnetic field strengths: 0 T (blue), 0.33 T (yellow), and 0.64 T (purple). Both the linear modulus and yield stress increase with increasing sample age and magnetic field strength.

Formation of Novel Solid Foams. Hierarchical porosity has been shown over the past decade to enhance the functionality of many different materials, including biomedical implants and catalysts.^{30, 31} Porous materials are currently being investigated across different research fields and can be generated using the following methods: solution casting, gel casting, particulate leaching, gas saturation, lithography, biotemplating, electrospinning as well as rapid prototyping (just to name a few).^{32, 33} Although not discussed in detail here, each of these processes possess drawbacks, mostly involving scalability or harsh processing conditions. What if there was a more scalable and simple method by which to produce materials with hierarchical porosity? Foams of varying stability and microstructure can be formed by tuning the characteristics of the particles employed in making the air-in-liquid dispersion. The wettability of particles employed in foam stabilization can be controlled by regulating the percentage of hydrophobic groups on their surfaces. Thus, particles of any chemical nature (metallic, polymeric, biopolymeric, etc.) can potentially be used to make Pickering foam as long as they have the correct wettability. In addition, foam structure (i.e. pore size, porosity, lamella thickness) can be tuned by varying the particle contact angle with the air-liquid interface, concentration of particle stabilizers in the foam, as well as by varying the content of other foam additives (polymers, surfactants, gelling agents, etc.).³⁴ Some examples of porous materials which have been generated using the direct foaming method include materials for scaffolds as well as catalyst supports.^{35, 36}

In preliminary experiments, we demonstrated that solid stimuli-responsive porous materials could be generated from the aqueous magnetic foams presented above. One popular method for producing porous solid materials from foams as well as colloidal dispersions of elongated/asymmetric particles is freeze-drying or lyophilization. Foams were poured directly from the blender jar into plastic 50 mL centrifuge tubes in which the samples were allowed to drain for ~ 30 mins. The drained liquid was extracted using a needle and the remaining foam stored at -80°C for preservation of structure prior to freeze-drying. Solid foams obtained after lyophilization demonstrated selectivity for oil absorption over water absorption owing to the hydrophobically-modified cellulose used to stabilize the aqueous magnetic foams (**Figure 16**). Solid foam samples could be manipulated using a permanent magnet subsequent to oil adsorption (**Figure 17**). This preliminary data demonstrates the versatility of biopolymeric particulate stabilizers for the production of solid functional materials from aqueous foams. Such solid porous materials can potentially be utilized for oil cleanup as well as collection of other hydrophobic contaminants. In addition, from the perspective of sustainability, the foams produced in this work have

the added advantage of being generated mostly from a renewable material. It is the hope of the authors that the results of this dissertation will contribute to a new generation of sustainable materials where naturally renewable sources are processed into colloidal structures with enhanced functionality, and are used in novel hybrid materials like those presented here.

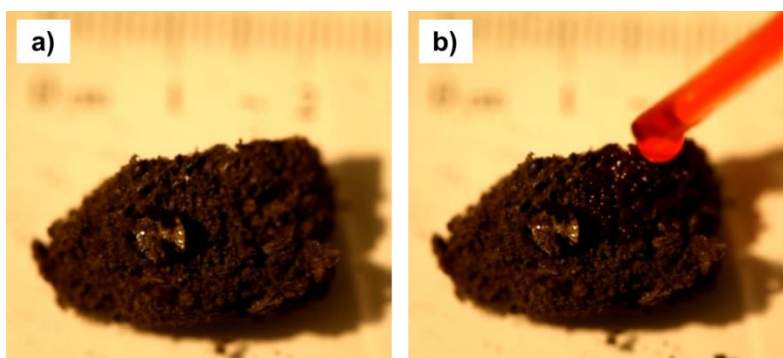


Figure 16. Solid magnetically-responsive foam stabilized by HPMCP. (a) Photograph of a water droplet atop of a solid magnetic foam sample. Notice that the droplet is not absorbed by the foam. (b) Photograph showing absorption of oil by the same foam sample (at top right corner of sample).

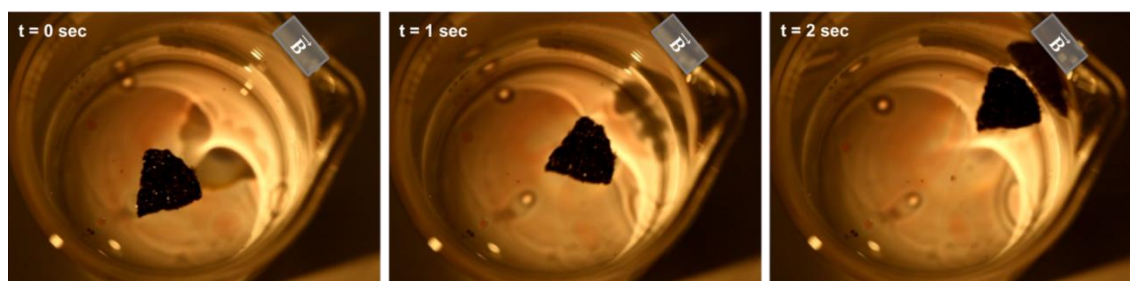


Figure 17. Series of photographs showing the migration of a solid foam sample toward the source of the applied magnetic field (subsequent to oil absorption).

Future Perspectives. The future work in this new directions may involve developing a quantitative technique by which to study single films of different ages, and to correlate the rheological properties of these films to the collapse behavior of the wet and dry foams. Additional work to refine the process for developing solid foams which could be manipulated using external stimuli may also follow. As mentioned in the past updates, we have published two articles pertaining to our work on formulating and characterizing the age-dependent collapse properties of magneto-Pickering foams. One article was published in *JACS* in 2011 and a second one was recently published in *Langmuir* in 2013.^{17, 18}

Development of Novel Multi-Stimuli Responsive Foams.

As described above, we generated photo-responsive foam by combining a thermally responsive polymer (12-hydroxystearic acid) with light absorbent particles (carbon black particles or CBP) in the continuous phase of a foam (**Figure 18**). Ethanolamine counterion was added to the 12-HSA mixture to control the temperature at which the fatty acid assembly will transition from tube-like structures to micelles. The stability of foams made with 12-HSA have already been characterized. In addition, it is well known that tubular assemblies of this specific fatty acid can produce very stable foams and that the stability of these foams can be tuned by changing the temperature of the system.³⁷ We first showed that the addition of CBP to the 12-HSA foam did not reduce the stability of the foam. In fact a CBP/12-HSA foam can remain stable for several months. Foam collapse was induced by illuminating the sample with a UV light. CBPs in the foam absorb the incident UV light and heat up to a temperature above that of the $T_{\text{transition}}$ of 12-HSA. This causes the fatty acid tubes in the foam to transition from tubules to micelles, resulting in foam collapse. We observed the photothermal collapse of the 12-HSA/CBP foams using an IR camera. Snapshots from the IR movie in **Figure**

19 show that under UV illumination, the temperature inside the foam reaches 50°C, which is > than the 12-HSA $T_{\text{transition}}$ of 45°C. The heating of the CBPs in the foam lamella above $T_{\text{transition}}$ causes the fatty acid assemblies in the foam to rearrange from tubes to micelles, resulting in foam collapse. The collapse properties of this foam system were evaluated as a function of system composition (**Fig. 20**). In brief, we found that the rate of foam collapse increased with increasing CBP concentration and decreasing water fraction in the foam lamella. In addition, we also observed that there was an optimal fatty acid concentration at which foam collapse was rapid, and that above this concentration, foam collapse slowed.

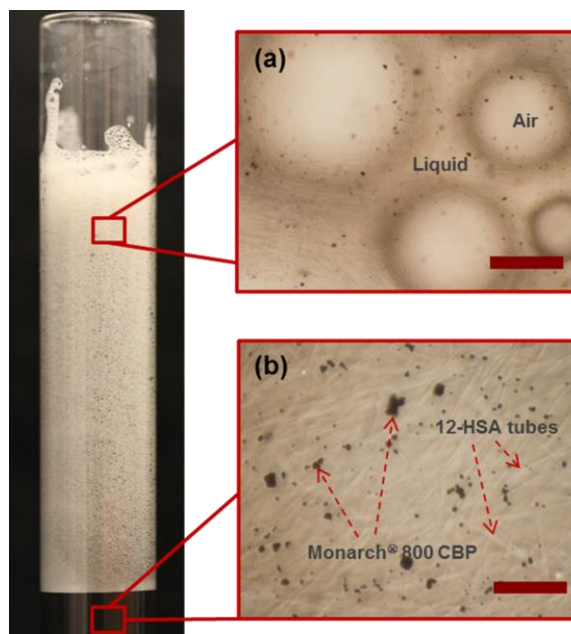


Figure 18. Photographs of a freshly-made foam with microscope images corresponding to the foam head and liquid drained out of the foam. **(a)** Micrograph of fresh foam showing thick foam films containing 12-HSA tubes and CBP. **(b)** 12-HSA tubes and carbon black particles in solution. The scale bar represents 50 μm .

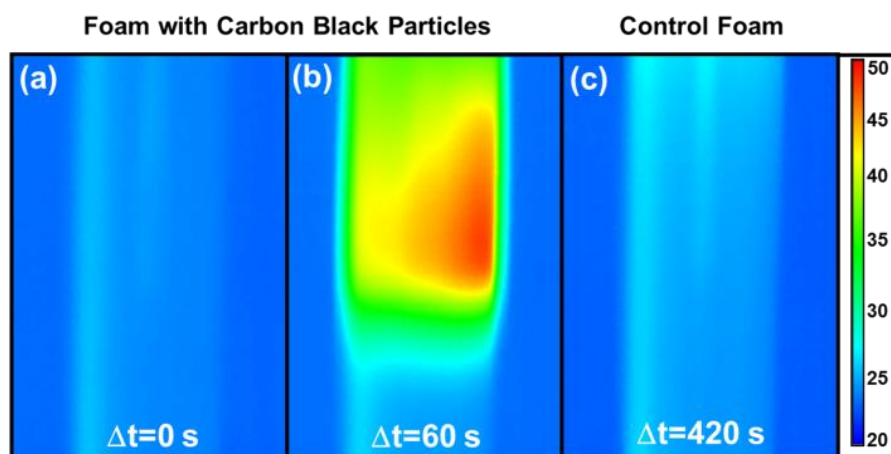


Figure 19. Snapshots extracted from IR movies showing the temperature profiles of a 12-HSA/CBP foam sample contained in a glass vessel **(a)** before irradiation with UV light, and **(b)** 60 seconds after UV light irradiation. **(c)** Control foam sample 7 minutes after UV light irradiation.

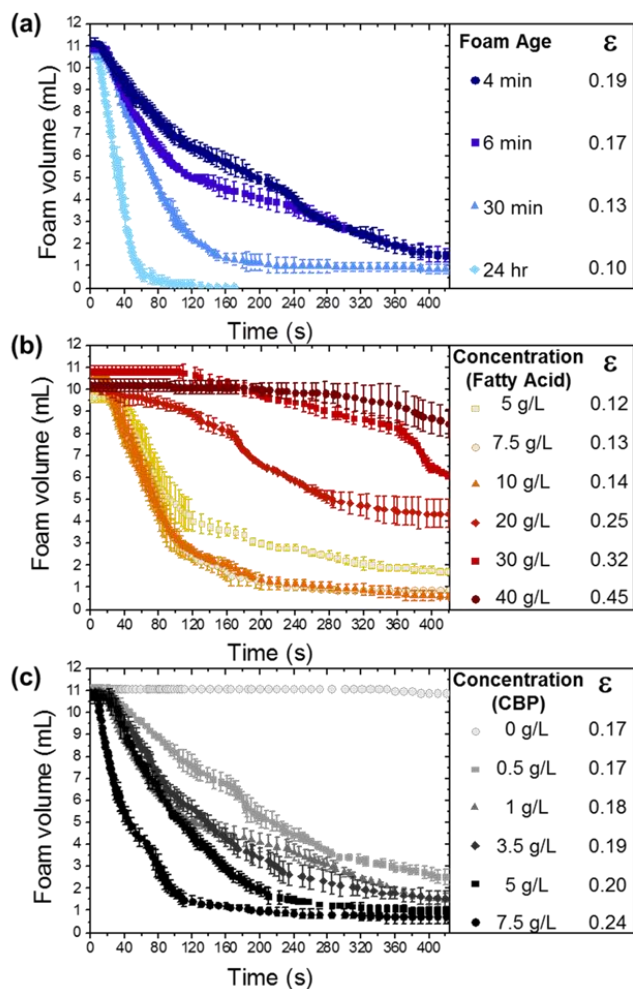


Figure 20. (a) Evolution of the foam head volume as a function of UV illumination time for foams of different ages (different water fractions due to pre-drainage times). (b) Evolution of foam volume as a function of the illumination time for foams containing different concentrations of 12-HSA with a fixed concentration of CBP (Monarch® 800) at 1 g/L. All samples were illuminated 10 minutes after the foam formation. (c) Evolution of the foam volume as a function of illumination time for foams with different concentrations of CBP (Monarch® 800) and a fixed 12-HSA concentration of 10 g/L. All samples were tested 6 minutes after the foam formation.

foam resulting from heat dissipation from the CBPs or metallic particles in the foam during the application of UV stimulus. This will not only help determine whether foam collapse is due to poor foam stabilization by nanometric-sized micelles, or Marangoni flows created as a result of the transition of 12-HSA from tubes to micelles; but can also potentially demonstrate how Marangoni flows can drive structural collapse in wet foams. In addition this, we also plan to formulate and demonstrate UV-responsive foamulsions. UV responsive foamulsions, which contain an additional liquid phase, can serve as potential reactant delivery vehicles in water remediation processes. Most of this work was published in *Chemical Science* in 2013, and was not only highlighted by the journal but also a news site.³⁷⁻³⁹

We hypothesized that this was because the viscosity of the fatty acid tube solution has to be high enough to trap a considerable amount of CBP inside the foam liquid channels, but at the same be low enough to form foams which are not very wet.

We also showed the 12-HSA and CBP foams could be destroyed using sunlight. This demonstrated the potential for making foams which are responsive to solar illumination. In addition, we tested how easily the method for making photothermal foam could be extended by using other types of light absorbent particles, such as metallic particles in place of CBPs. For this test, we used the same carbonyl iron particles which had been utilized in the magneto-Pickering foam project. We tested the response of 12-HSA foam containing carbonyl iron to various stimuli and saw that it was not only photo-responsive, but also thermally and magnetically responsive (**Figure 21**). This account of a multi-stimuli responsive foam is the first account which has been reported to our knowledge. In summary, we have produced a foam which is responsive to thermal, light as well as magnetic stimulus from inexpensive materials. Not only is the foam stable until exposed to temperature, light or magnetic stimulus above a certain threshold; but, in the case of foam collapse by UV illumination, the extent of collapse can be controlled by simply removing the UV stimulus. In addition, foams can easily be regenerated after collapse.

Future Work. Since the exact mechanism by which the 12-HSA/CBP foams collapse in response to UV illumination remains unclear, we hope to perform studies which can help shed more light on this aspect of the system. To do this, we plan to study thermal gradients in the

Formation and Application of Lignin Particles for Colloidal Stabilization. Lignin, whose name is derived from the Latin word “*lignum*” for wood, is the most abundant aromatic compound found in nature.⁴⁰ It is a copious natural resource and has many potential uses as a dispersant, chemical precursor, and as a constituent of composite materials.^{40, 41} The exact chemical structure of natural lignin may vary, but it is known that lignin is aggregated *in vivo* in the cell wall of woody plants.⁴² There are three main monolignols (p-coumaryl alcohol, coniferyl alcohol, and sinapyl alcohol) which make up the lignin macromolecule; the ratio of these three monolignols vary with the source from which the lignin is obtained.^{43, 44, 45} In addition, the processing conditions, which natural lignin undergoes (i.e. sulfite pulping, Kraft pulping, steam explosion) will determine its end functionality as well as molecular weight (MW).⁴⁶ Unlike its biological counterpart, cellulose, lignin is amorphous and does not exhibit any structurally-generated optical properties.^{40, 47} The inhomogeneity in the structure of natural lignin across different plant species translates to inefficiencies in its separation from cellulose. This is particularly problematic in the biofuels industry where lignin and hemicelluloses need to be removed to recover cellulose from plants at high purity.⁴⁸ Thus, there has been much effort devoted to understanding the colloidal properties of natural as well as modified lignins (i.e. alkaline lignin and lignosulfonates) to design more effective methods by which to separate lignin from cellulosic biomass.^{45, 46, 49-57} More recently, research into different forms of lignins have been fueled by the motivation to utilize this renewable material to fabricate value-added commodities by understanding the properties and elucidating the potential of these natural aromatic compounds as molecular surfactants, particulate emulsifiers, and as replacements for petroleum-based synthetic polymers.^{40, 58-61}

One modified form of lignin which has been a popular subject of study over the past few decades is Kraft lignin (KL). Kraft lignin (aka alkaline lignin) is a byproduct of the Kraft pulping process, which is used to make paper. Every year, ~ 5 million tons of KL is generated by the paper industry and ~ 98 % of it is burned as fuel in paper mills; ~ 2% is utilized for the production of value-added products.⁴⁰ KL is often studied, not only because it is an abundant and inexpensive byproduct, but because the colloidal properties of this type of lignin can lead to a better understanding of alkaline-based separation methods for cellulose purification in the biofuel as well as pulp and paper industries. In the work presented here, foams stabilized by KL particles are generated and characterized. Synthesis parameters are tuned so that particles with improved foam stabilizing attributes may be formed. Such foams could have potential applications in water remediation and as value-added consumer products.

Lignin particle dispersions containing anisotropically-shaped particles, as well as a microgel/mesh-like network were prepared using a water-based shear process (**Figure 22**). First, Indulin®AT was dissolved in deionized water at pH ~ 12 to prepare a stock solution. Particles were synthesized by injecting the KL solution into a low pH (~ 2) medium under shear (Cole-Palmer Servodyne Mixer, 1500 rpm, 3 min) to induce the precipitation of the KL biopolymer out of solution in the form of particles. In this work, particle/microgel products generated via this process are termed “reformed particles”. The dissolution of KL with an increase in solution alkalinity and precipitation out of solution in acidic conditions is a well-known phenomenon and has been studied by other authors.^{50, 55, 62-65} KL foams were generated by aerating particle and microgel dispersions in a professional blender running at 15000 rpm for 60 seconds (Oster Model 4242, Sunbeam Products, Inc., Boca Raton, FL). Samples were subsequently poured from the blender jar into graduated cylinders for observation.

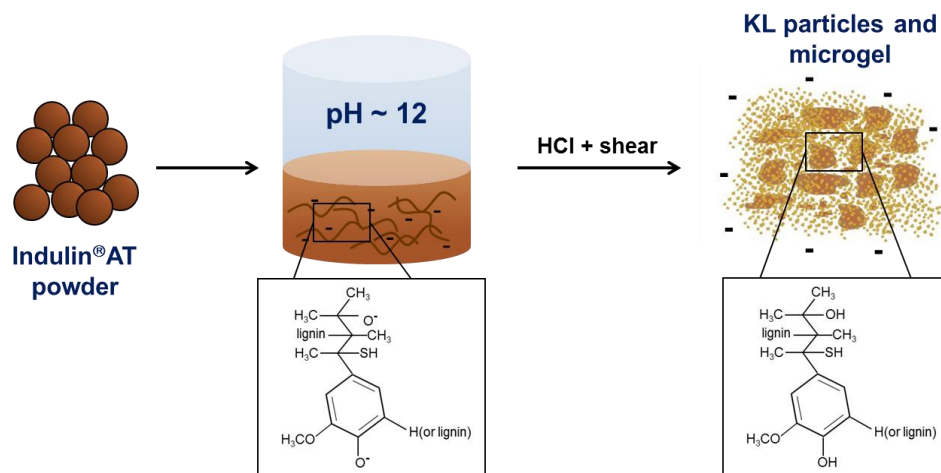


Figure 22. Schematic of procedure for generation of KL particle/microgel mixture. Corresponding KL structures show the ionization of hydroxyl groups during the different stages of the reformation process.

Particles generated using the water-based shear process described above are polydisperse in size (microns), and those which are large enough for visualization under optical microscopy are either rod-shaped or plate-like (**Figure 23**). From previous studies it is well known that a decrease in solution pH results in the protonation of phenolic and aliphatic hydroxyl groups on the KL macromolecule. This is followed by hydrogen bonding in the loose surface regions of lignin between protonated hydroxyl groups, resulting in polymer aggregation to form particles.^{46, 50-53, 66} Despite the varying shapes of lignin particles produced, many of the larger particles are plate-like; this characteristic can most likely be attributed to π - π stacking between the aromatic rings in the lignin macromolecule during the precipitation of KL polymer out of solution.⁵⁰ One noticeable difference between the reformed particles and Indulin® AT powder that can be seen in **Figure 23** is that non-reformed lignin particles tend to form dense aggregates. These particles also show a high level of contrast with the aqueous background. The reformed particles on the other hand, have low contrast with the background and form voluminous aggregates. From these images, it appears that the process of reformation dispersed the lignin polymer that was condensed in the original particles into voluminous low-density aggregates.

Recently, Petridis et al. used small angle neutron scattering (SANS) in conjunction with molecular simulations to demonstrate the fractal nature of natural lignin aggregates on the angstrom level.⁴² The authors showed that the aggregates were highly folded, very compact and that they react favorably with water (despite the hydrophobicity of natural lignin). This is mostly a result of hydrogen bonding between water molecules and lignin hydroxyl groups.^{42, 62} We should also expect to observe this hydration behavior in Kraft lignin,

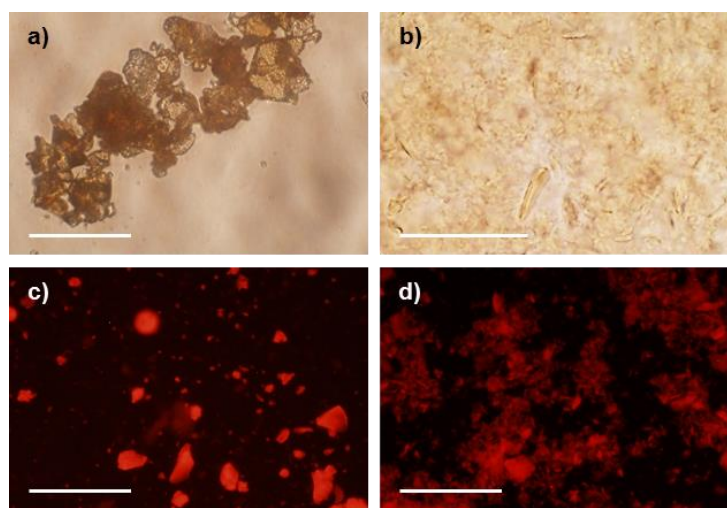


Figure 23. Micrographs of non-reformed (a, c) and reformed particles (b, d). Scale bar = 100 μm .

which contains more hydroxyl groups - as well as thiol and methoxy groups - than natural lignin. Thus, it can be hypothesized that the voluminous structure of the reformed particles is partly due to hydration.

While examining the particle suspensions via optical microscopy, a smaller population of particles can be visualized qualitatively but not quantitatively. For characterization of particle sizes in the smaller population of precipitated KL, TEM was employed. However, from the transmission electron micrographs, one cannot see any distinct particles but rather a mesh-like network containing KL polymer (**Figure 24**). It is possible that KL nanoparticles formed aggregates during TEM sample preparation, or that the “microgel” observed under optical microscopy is a network of KL polymers agglomerated through hydrogen-bonding subsequent to the reformation process.⁵³

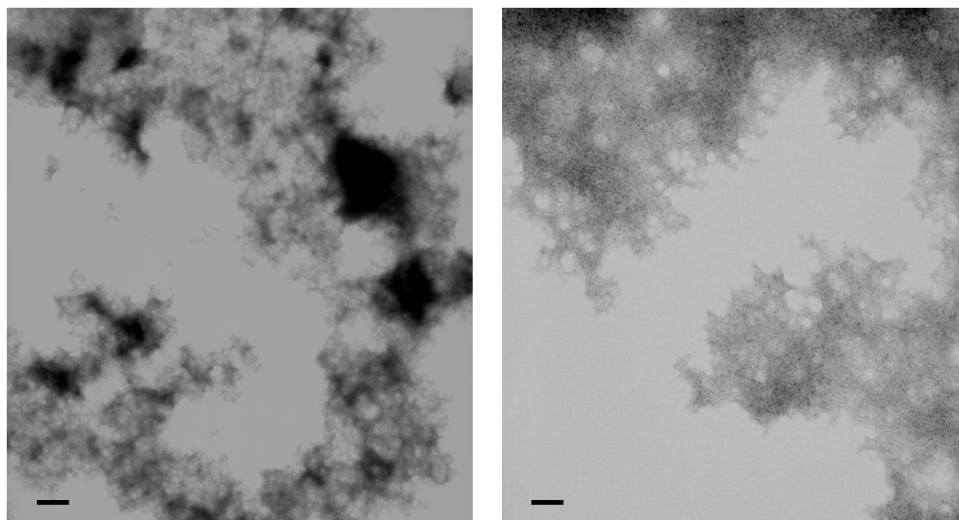


Figure 24. Transmission electron micrographs of Indulin® AT microgel formed from a water-based shear method at pH ~ 1.3. (*Left*) TEM image of KL aggregates at 5000× magnification. Scale bar = 1 μm . (*Right*) TEM image of KL aggregates at 50,000× magnification. Scale bar = 100 nm.

To elucidate whether the water-based shear reformation process changed the surface charge of KL particles, zeta-potential measurements were performed (**Figure 25**). Data from these experiments show that reformed particles are slightly less charged than non-reformed particles, meaning that they are, from an electrostatic point of view, better foam stabilizers than the non-reformed particles. ζ -potentials greater than ± 25 mV are generally desired for colloidal stability. However, for foam stabilization by particles, values less than ± 25 mV are desired.⁶⁰ At these values, there would be particle adsorption at the air-liquid interface without strong lateral electrostatic repulsion between particles. In **Figure 25**, it can be seen that as pH decreases, ζ -potential increases for both the reformed and non-reformed particles until pH ~ 5. At this point, the ζ -potential of the reformed particle system becomes unmeasurable, and that for the non-reformed particle system begins to decrease. An increase in ζ -potential with increasing pH for pHs < 5 followed by a leveling off of ζ -potential for pHs > 5 has also been observed by other authors for KL.⁴⁹ During the measurements of ζ -potential, it was discovered that the solubility of lignin is altered after the reformation process. Curves representing the ζ -potential of the reformed particles terminated at pH ~ 5. This was the pH after which the Zetasizer instrument did not detect the presence of any particles. For the non-reformed particle system, it was not until a pH value of ~ 11 that the Zetasizer ceased to detect the presence of particles.

Measurement of sample absorbance for supernatants from reformed and non-reformed particle samples confirmed a change in solubility following the water-based shear process (**Figure 26**). The pH at which there is a critical change in the solubility of the particles determined using spectroscopy correlates well with the solubility behavior observed from ζ -potential experiments (pH \sim 5). The absorbance study for the KL system demonstrates that while reformed KL particles dissolve back into solution at lower pHs, they also more readily precipitate out of solution at pH values less than 5. In **Figure 26**, it can be seen that at pHs below 5, the concentration of lignin in the supernatant of the reformed particle dispersion is much lower than that in the non-reformed particle dispersion. This means that more polymer was precipitated out of solution during the reformation process in the form of particulates. At pH \sim 2, the concentration of KL in the supernatant for the non-reformed particle suspension is 7 \times higher than for the reformed particle suspension. These data imply that in the reformed particle system, 7 times more lignin polymer is precipitated out of solution.

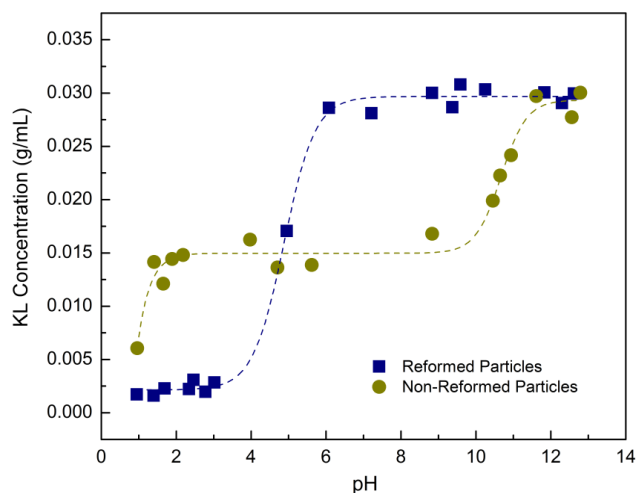


Figure 26. Solubility of reformed and non-reformed particles as a function of pH. At pH \sim 2, reformed particle system is 7 times less soluble than non-reformed particle system. Reformed particles begin dissolving back into solution at pH \sim 5 whereas non-reformed particles do not fully dissolve until pH \sim 12.

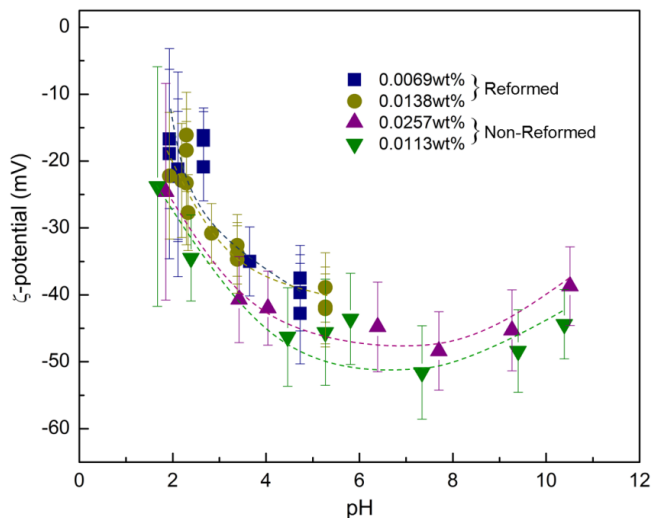


Figure 25. ζ -potential vs. pH for reformed and non-reformed Indulin®AT particles. For all samples measured, absolute ζ -potential increases with an increase in sample pH until pH \sim 5. After this point, it decreases slightly with increasing pH for the non-reformed particle samples and becomes unmeasurable for the reformed samples.

The ability of the reformed particles to stabilize foam was evaluated and compared to that of non-

reformed KL particles. Although foam stabilization by KL has not been reported to our knowledge, the stabilization of various types of emulsions using KL has been evaluated by researchers.^{54, 56-58, 60, 67, 68} Foams were generated as described in the Methods Section. By monitoring foam volume and liquid drainage over time, we find reformed lignin particles to be more efficient stabilizers than the original KL particulates at the same concentration and pH conditions (**Figure 27**). Foams made using the reformed particles were stable for days and even weeks whereas those stabilized using the original lignin powder collapsed after \sim 1 day. The increased stability imparted by the reformed particles on the foam structure could be a consequence of the reformed particles being more voluminous than non-reformed particles. Micrographs of foam bubbles stabilized by reformed and non-reformed particles are shown in the inset of **Figure 27**.

Observations of foam bubbles stabilized by non-reformed versus reformed particles indicate that while particles from the non-reformed KL system do adsorb at the air-liquid interface, the coverage of the bubble surfaces is sparse, making the system more prone to destabilization by mechanisms such as coarsening and bubble coalescence. Reformed particles, however, not only adsorb at the air-water interface, but also offer more complete surface coverage to the bubbles in the foam system. In addition to providing a greater amount of coverage, the particles appear to have aggregated into a gel-like structure at the air-liquid interface - sterically stabilizing the foam bubbles against coalescence and coarsening through the formation of thicker, more viscous films in the foam lamella. Foam stability was also studied as a function of KL concentration as well as the pH of the foaming medium (**Figures 28 and 29**).

From **Figures 28 and 29**, it can be seen that increasing the concentration of lignin in the foam resulted in higher foam stability, and that decreasing the pH of the foaming medium also resulted in an increase in foam stability. Both of these conclusions could be summarized as follows: higher foam stability results from an increase in the surface coverage of foam bubbles by particles. An increase in the concentration of lignin used for foam generation also resulted in an increase in the number of particles available for foam stabilization. Similarly, since KL dissolves at high pH and precipitates out of solution at low pH, more KL is precipitated out of solution at lower pH values, resulting in more material available for foam stabilization. This pH dependent foam stability which was observed in the KL system can be utilized to generate foams in which stability can be tuned by changes in pH. In preliminary experiments, it was observed that foams generated using reformed KL particles can be destabilized by increasing the pH of the continuous phase using NaOH (to dissolve KL particles). Decreasing medium pH while foaming results again in stable KL foam. To gain a better understanding as to how the effective volumes of the reformed and non-reformed particles correlate to differences observed in foam stability in these two systems, the volumes of both particle dispersions were monitored at the same pH and KL concentration over time. It was observed that reformed particles compacted slowly over time while the non-reformed particles settled out of solution to a volume of $\sim 300 \mu\text{L}$ after one day (**Figure 30**). Even after 36 days, reformed particles had ~ 30 times larger volume (mL) and ~ 40 times larger specific volume (mL/g KL) than the non-reformed KL particles.

One detail which was observed during the experiments was that the supernatant above the precipitated non-reformed particle mass was much more turbid than the supernatant above the reformed particle agglomerate. From this, we can infer that there is more lignin polymer dissolved in the supernatant of the non-reformed particle sample. By measuring the absorbance of the supernatant in the non-reformed and reformed particle systems, it was found that the amount of KL remaining in solution in the reformed and non-reformed samples at pH ~ 2 differs by a factor of ~ 7 (**Figure 26**). Although this elucidates one factor contributing to the volume increase in the reformed KL system, there is still a 23-fold increase in volume resulting from the reformation process which still has to be accounted for. This volume increase is likely caused by differences in KL particle structure between the two systems. The reformation process results in a redistribution of lignin polymer into smaller-sized aggregates than that

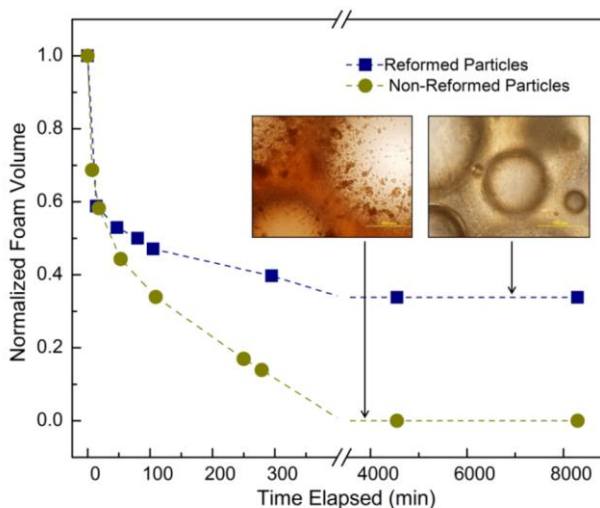


Figure 27. Normalized foam volume vs. time for foam stabilized by reformed and non-reformed particles. (*Inset*) Micrographs showing KL particles adsorbed at the air-water interface. KL concentration = 0.7 wt% and pH ~ 2 for foams. Foams made with reformed particles remain stable for a longer period of time.

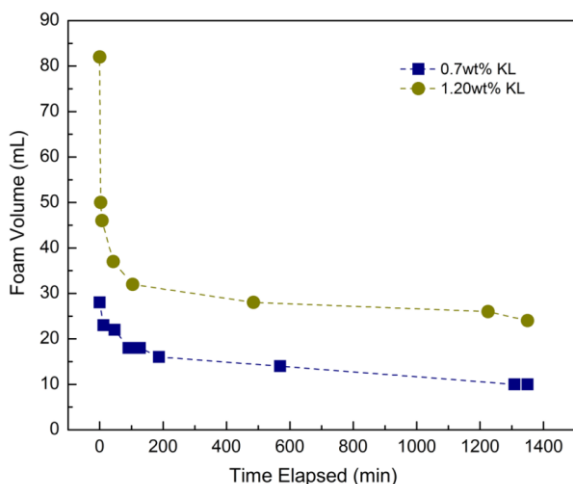


Figure 28. Plot of foam volume vs. time for samples stabilized by different concentrations of KL (pH ~ 2). Foams made with suspensions containing higher concentrations of KL maintain larger foam volumes and have greater stability against creaming.

as in the hydration layer around particle aggregates. By using thermogravimetric analysis or a similar dye adsorption study as that employed by Frangville et al. in the future, the location of captured water molecules in the reformed KL system may be determined.³³ In summary, the loosely-aggregated, voluminous structure of the reformed particles in solution can be attributed to two main factors – increased precipitation of KL polymers out of solution and the entrainment of H₂O molecules in the aggregated reformed particle matrix. The increase in the effective volume occupied by KL after the reformation process contributes greatly to the ability of the reformed particles to stabilize foams. In summary, we have re-engineered KL particulates, which are themselves emulsifiers, into more efficient foam stabilizers by reforming the particles using a water-based shear process. We characterized the effect of the reformation process on the surface charge and structure of KL particles. The ζ -potential of the particles was found to change with pH and was slightly lower following the reforming process. The procedure for generating reformed KL particles was found to increase the volume of the original particles by ~ 30 times, which resulted in an enhanced ability of reformed KL to sterically stabilize foams and emulsions. The highest foam stability was recorded at low pH (~ 2), corresponding to a ζ -potential of approximately -20 mV. Thus, we have developed an efficient, environmentally-friendly method by which to increase the effective volume of lignin particles, which after the reformation process show enhanced properties as foam and potentially, emulsion stabilizers. A manuscript for this work is in preparation.

found in the original system. Aggregates in the reformed particle system, which are not only smaller in size but also less dense than the particles in the original system, can allow for a higher degree of hydration in the KL particle matrix. During measurement of particle volume, it was also observed that the loosely-packed reformed particle aggregates, which maintain a higher effective volume in solution over time, retain more water than the non-reformed particle aggregates. For a system containing aggregated KL nanoparticles, Frangville and coworkers determined through a dye adsorption study that the active surface area of their NPs were 2.3 times that estimated from the measured hydrodynamic radius.³³ From this, the authors concluded that the nanoparticles themselves were porous. Likewise, the micron-sized particles in this system could also be porous, facilitating hydration of the KL reformed particle mass. Additionally, water molecules can be captured in the areas between KL particles during aggregate formation, as well

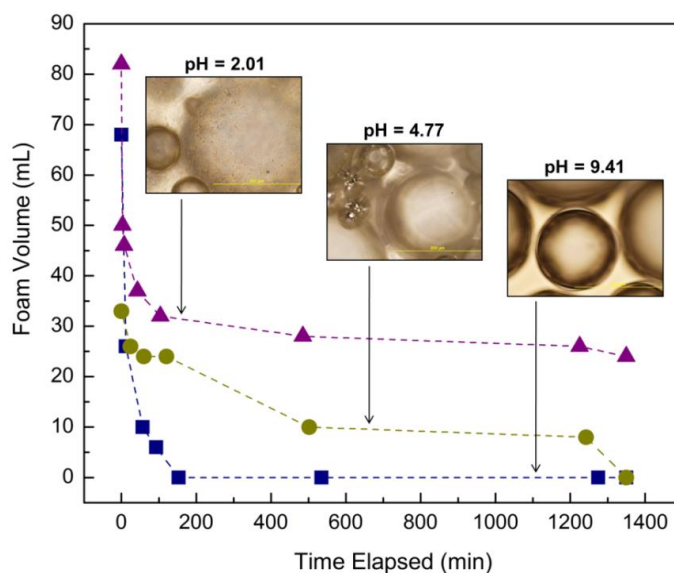


Figure 29. Foam volume vs. time for KL foam samples stabilized by particles generated at different pH conditions. Foam stability increases with decreasing pH due to the presence of more KL particles at lower pHs. KL concentration in foams = 1.20 wt%.

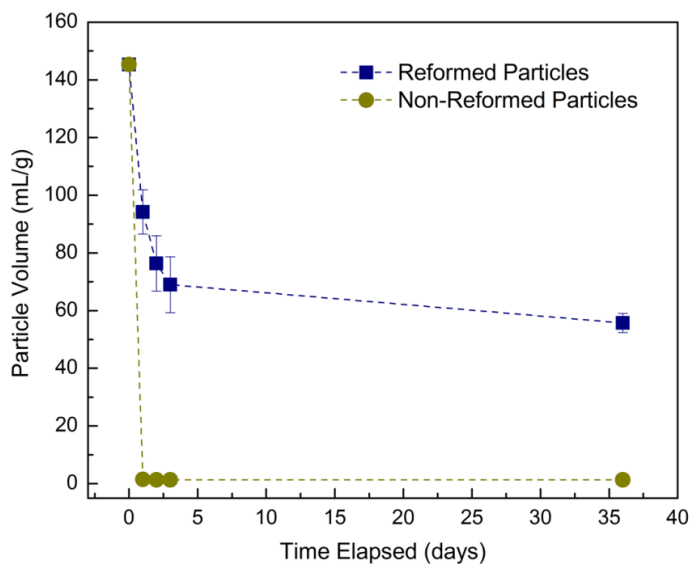


Figure 30. Specific volume of reformed and non-reformed particles as a function of time in aqueous media. Reformed particles compress slower in H₂O than non-reformed particles. Concentration of KL in suspensions ~ 0.7 wt% and pH ~ 2.

References cited

- Pickering, S. U., Emulsions. *J. Chem. Soc.* **1907**, 91, 2001-2021.
- Ramsden, W., Separation of Solids in the Surface-Layers of Solutions and 'Suspensions' (Observations on Surface-Membranes, Bubbles, Emulsions, and Mechanical Coagulation). *Proc. R. Soc. London* **1903**, 72, 156-164.
- Gonzenbach, U. T.; Studart, A. R.; Tervoort, E.; Gauckler, L. J., Ultrastable Particle-Stabilized Foams. *Angew. Chem. Int. Ed.* **2006**, (45), 3526-3530.
- Hunter, T. N.; Pugh, R. J.; Franks, G. V.; Jameson, G. J., The Role of Particles in Stabilising Foams and Emulsions. *Adv. Colloid Interface Sci.* **2008**, 137, 57-81.
- Cervantes-Martinez, A.; Rio, E.; Delon, G.; Saint-Jalmes, A.; Langevin, D.; Binks, B. P., On the Origin of the Remarkable Stability of Aqueous Foams Stabilised by Nanoparticles: Link with Microscopic Surface Properties. *Soft Matter* **2008**, 4, 1531-1535.
- Wege, H. A.; Kim, S.; Paunov, V. N.; Zhong, Q.; Velev, O. D., Long-Term Stabilization of Foams and Emulsions with In-Situ Formed Microparticles from Hydrophobic Cellulose. *Langmuir* **2008**, 24, 9245-9253.
- Kim, S.; Barraza, H.; Velev, O. D., Intense and Selective Coloration of Foams Stabilized with Functionalized Particles. *J. Mater. Chem.* **2009**, 19, 7043-7049.
- Cervin, N. T.; Andersson, L.; Ng, J. V. B. S.; Olin, P.; Bergström, L.; Wågberg, L., Lightweight and Strong Cellulose Materials Made from Aqueous Foams Stabilized by Nanofibrillated Cellulose. *Biomacromolecules* **2013**, 14, 503-511.
- Zoppe, J. O.; Venditti, R. A.; Rojas, O. J., Pickering Emulsions Stabilized by Cellulose Nanocrystals Grafted with Thermo-responsive Polymer Brushes. *J. Colloid Interface Sci.* **2012**, 369, 202-209.
- Klemm, D.; Heublein, B.; Fink, H.-P.; Bohn, A., Cellulose: Fascinating Biopolymer and Sustainable Raw Material *Angew. Chem. Int. Ed.* **2005**, 44, 3358-3393.
- Ougiya, H.; Watanabe, K.; Morinaga, Y.; Yoshinaga, F., Emulsion-stabilizing Effect of Bacterial Cellulose *Biosci. Biotech. Biochem.* **1997**, 61, 1541-1545.
- Kalashnikova, I.; Bizot, H.; Cathala, B.; Capron, I., New Pickering Emulsions Stabilized by Bacterial Cellulose Nanocrystals. *Langmuir* **2011**, 27, 7471-7479.
- Jin, H.; Zhou, W.; Cao, J.; Stoyanov, S. D.; Blijdenstein, T. B. J.; de Groot, P. W. N.; Arnaudov, L. N.; Pelan, E. G., Super Stable Foams Stabilized by Colloidal Ethyl Cellulose Particles. *Soft Matter* **2012**, 8, 2194-2205.
- Wege, H. A.; Kim, S.; Paunov, V. N.; Zhong, Q.; Velev, O. D., Long-Term Stabilization of Foams and Emulsions with In-Situ Formed Microparticles from Hydrophobic Cellulose. *Langmuir* **2008**, 24, 9245-9253.
- Patel, A. R.; Drost, E.; Blijdenstein, T. B. J.; Velikov, K. P., Stable and Temperature-Responsive Surfactant-Free Foamulsions with High Oil Volume Fraction *Chem. Phys. Chem.* **2012**, 13, 3741-4002.
- Kim, S.; Barraza, H.; Velev, O. D., Intense and Selective Coloration of Foams Stabilized with Functionalized Particles. *J. Mater. Chem.* **2009**, 19, 7043-7049.
- Lam, S.; Blanco, E.; Smoukov, S. K.; Velikov, K. P.; Velev, O. D., Magnetically Responsive Pickering Foams *J. Am. Chem. Soc.* **2011**, 133, 13856-13859.
- Blanco, E.; Lam, S.; Smoukov, S. K.; Velikov, K. P.; Khan, S. A.; Velev, O. D., Stability and Viscoelasticity of Magneto-Pickering Foams *Langmuir* **2013**, 29, 10019-10027.
- Fameau, A. L.; Saint-Jalmes, A.; Cousin, F.; Houssou, B. H.; Novales, B.; Navailles, L.; Nallet, F.; Gaillard, C.; Boue, F.; Douliez, J. P., Smart Foams: Switching Reversibly Between Ultrastable and Unstable Foams. *Angew. Chem. Int. Ed.* **2011**, 50, 8264-8269.
- Velikov, K. P.; Velev, O. D., Stabilization of Thin Films, Foams, Emulsions and Bifluid Gels with Surface-active Solid Particles. In *Colloid Stability and Application in Pharmacy*, Tadros, T. F., Ed. Wiley-VCH Publ.: Weinheim, 2007; pp 277-306.

21. Rullier, B.; Axelos, M. A. V.; Langevin, D.; Novales, B., B-lactoglobulin Aggregates in Foam Films: Correlation Between Foam Films and Foaming Properties *Journal of Colloid and Interface Science* **2009**, 336, 750-755.
22. Rullier, B.; Axelos, M. A. V.; Langevin, D.; Novales, B., B-lactoglobulin Aggregates in Foam Films: Effect of the Concentration and Size of the Protein Aggregates *J. Colloid. Interf. Sci.* **2010**, 343, 330-337.
23. Murray, B. S.; Durga, K.; Yusoff, A.; Stoyanov, S. D., Stabilization of Foams and Emulsions by Mixtures of Surface Active Food-grade Particles and Proteins. *Food Hydrocolloids* **2011**, 25, 627-638.
24. Lam, S.; Velikov, K. P.; Veleev, O. D., Pickering Stabilization of Foams and Emulsions with Particles of Biological Origin. *Curr. Opin. Colloid Interface Sci.* **2014**.
25. Banhart, J.; García-Moreno, F.; Hutzler, S.; Langevin, D.; Liggieri, L.; Miller, R.; Saint-Jalmes, A.; Weaire, D., Foams and Emulsions in Space *Europhys. News* **2008**, 39, 26-28.
26. Saint-Jalmes, A.; Langevin, D., Time evolution of aqueous foams: drainage and coarsening. *J. Phys.: Condens. Matter* **2002**, 14, 9397-9412.
27. Rich, J. P.; Doyle, P. S.; McKinley, G. H., Magnetorheology in an Aging, Yield Stress Matrix Fluid. *Rheol Acta* **2012**, 51, 579-593.
28. Jolly, M. R.; Bender, J. W.; Carlson, J. D., Properties and Applications of Commercial Magnetorheological Fluids In *Proc. SPIE 3327*, Davis, L. P., Ed. San Diego, CA 1998; pp 262-275.
29. Satoh, A.; Chantrell, R. W.; Kamiyama, S.-I.; Coverdale, G. N., Two-Dimensional Monte Carlo Simulations to Capture Thick Chainlike Clusters of Ferromagnetic Particles in Colloidal Dispersions *J. Colloid Interface Sci.* **1996**, 178, 620-627.
30. Jones, J. R.; Lee, P. D.; Hench, L. L., Hierarchical Porous Materials for Tissue Engineering. *Phil. Trans. R. Soc. A* **2006**, 364, 263-281.
31. Yokoi, T.; Tatsumi, T., Hierarchically Porous Materials in Catalysis In *Hierarchically Structured Porous Materials: From Nanoscience to Catalysis, Separation, Optics, Energy, and Life Science.*, 1 ed.; Su, B. L.; Sanchez, C.; Yang, X. Y., Eds. Wiley-VCH Verlag GmbH & Co. KGaA.: Germany, 2012.
32. Agrawal, C. M.; Ray, R. B., Biodegradable Polymeric Scaffolds for Musculoskeletal Tissue Engineering. *J. Biomed. Mater. Res.* **2001**, 55, 141-150.
33. Zhu, N.; Chen, X., Biofabrication of Tissue Scaffolds In *Advances in Biomaterials Science and Biomedical Applications* Pignatello, R., Ed. InTech: 2013.
34. Juillerat, F. K.; Gonzenbach, U. T.; Elser, P.; Studart, A. R.; Gauckler, L. J., Microstructural Control of Self-Setting Particle-Stabilized Ceramic Foams. *J. Am. Ceram. Soc.* **2011**, 94, 77-83.
35. Juillerat, F. K.; Engeli, R.; Jerjen, I.; Sturzenegger, P. N.; Borcard, F.; Jeanneret, L. J.; Gerber-Lemaire, S.; Gauckler, L. J.; Gonzenbach, U. T., Synthesis of Bone-like Structured Foams. *J. Eur. Ceram. Soc.* **2013**, 33, 1497-1505.
36. Studart, A. R.; Nelson, A.; Iwanovsky, B.; Kotyrba, M.; Kundig, A. A.; Dalla Torre, F. H.; Gonzenbach, U. T.; Gauckler, L. J.; Löffler, J. F., Metallic Foams From Nanoparticle-stabilized Wet Foams and Emulsions. *J. Mater. Chem.* **2012**, 22, 820-823.
37. Fameau, A. L.; Lam, S.; Veleev, O. D., Multi-stimuli Responsive Foams Combining Particles and Self-Assembling Fatty Acids *Chem. Sci.* **2013**, 4, 3874-3881.
38. <http://www.chemeurope.com/en/news/144727/destroying-stable-foams-on-demand.html>
39. <http://www.rsc.org/chemistryworld/2013/08/destroy-stable-foam-demand>
40. Calvo-Flores, F. G.; Dobado, J. A., Lignin as Renewable Raw Material. *ChemSusChem* **2010**, 3, 1227-1235.
41. Beis, S. H.; Mukkamala, S.; Hill, N.; Joseph, J.; Baker, C.; Jensen, B.; Stemmler, E. A.; Wheeler, M.; Frederick, B. G.; van Heiningen, A.; Berg, A. G.; DeSisto, W. J., Fast Pyrolysis of Lignins *BioResources* **2010**, 5, 1408-1424.

42. Petridis, L.; Pingali, S. V.; Urban, V.; Heller, W. T.; O'Neil, H. M.; Foston, M.; Ragauskas, A.; Smith, J. C., Self-similar multiscale structure of lignin revealed by neutron scattering and molecular dynamics simulation. *Phys. Rev. E* **2011**, 83, 061911 (1) – (4).
43. dos Santos Abreu, H.; do Nascimento, A. M.; Maria, M. A., Lignin Structure and Wood Properties *Wood and Fiber Sci.* **1999**, 31, 426-433.
44. Sarkanen, K. V.; Ludwig, H., *Lignins*. Wiley-Interscience, Inc.: New York, 1971.
45. Rojas, O. J.; Salager, J. L., Surface Activity of Bagasse Lignin Derivatives Found in the Spent Liquor of Soda Pulp Plants. *Tappi J.* **1994**, 77, 169-174.
46. Lindstrom, T., The Colloidal Behaviour of Kraft Lignin. *Colloid. Polym. Sci.* **1979**, 257, 277-285.
47. Sarkanen, K. V., *The Chemistry of Wood* Interscience Publishers: New York 1963.
48. Notley, S. M.; Norgren, M., Adsorption of a Strong Polyelectrolyte to Model Lignin Surfaces *Biomacromolecules* **2008**, 9, 2081-2086.
49. Hubbe, M. A.; Rojas, O. J., Colloidal Stability of Cellulosics *BioResources* **2008**, 3, 1419-1491.
50. Woerner, D. L.; McCarthy, J. L., Lignin. 24. Ultrafiltration and Light-Scattering Evidence for Association of Kraft Lignins in Aqueous Solutions. *Macromolecules* **1988**, 21, 2160-2166.
51. Sarkanen, S.; Teller, D. C.; Stevens, C. R.; McCarthy, J. L., Lignin. 20. Associative Interactions between Kraft Lignin Components. *Macromolecules* **1984**, 17, 2588–2597.
52. Sarkanen, S.; Teller, D. C.; Hall, J.; McCarthy, J. L., Lignin. 18. Associative Effects Among Organosolv Lignin Components. *Macromolecules* **1981**, 14, 426-434.
53. Rudatin, S.; Sen, Y. L.; Woerner, D. L., Association of Kraft Lignin in Aqueous Solution In *Lignin*, Glasser, W. e. a., Ed. American Chemical Society: Washington, DC, 1989; pp 144-154.
54. Rojas, O. J.; Bullón, J.; Ysambertt, F.; Forgiarini, A.; Salager, J. L.; Argyropoulos, D. S., Lignins as Emulsion Stabilizers In *Materials, Chemicals, and Energy from Forest Biomass*, Argyropoulos, D. S., Ed. American Chemical Society: 2007; Vol. 954, pp 182–199.
55. Norgren, M.; Edlund, H.; Wagberg, L., Aggregation of Lignin Derivatives Under Alkaline Conditions. Kinetics and Aggregate Structure. *Langmuir* **2002**, 18, 2859-2865.
56. Gundersen, S. A.; Ese, M. H.; Sjoblom, J., Langmuir Surface and Interface Films of Lignosulfonates and Kraft Lignins in the Presence of Electrolyte and Asphaltenes: Correlation to Emulsion Stability. *Colloids Surf., A* **2001**, 182, 199-218.
57. Afanas'ev, N. I.; Selyanina, S. B.; Selivanova, N. V., Stabilization of the Oleic Acid–Water Emulsion with Various Kraft Lignins. *Russ. J. Appl. Chem.* **2008**, 81, 1851-1855.
58. Yang, Y.; Wei, Z.; Wang, C.; Tong, Z., Lignin-based Pickering HIPEs for Macroporous Foams and Their Enhanced Adsorption of Copper(II) Ions. *Chem. Commun.* **2013**, 49, 7144 - 7146.
59. Stevens, E. S.; Klamczynski, A.; Glenn, G. M., Starch-lignin Foams. *eXPRESS Polym. Lett.* **2010**, 4, 311–320.
60. Wei, Z.; Yang, Y.; Yang, R.; Wang, C., Alkaline Lignin Extracted from Furfural Residues for pH-responsive Pickering Emulsions and Their Recyclable Polymerization *Green Chem.* **2012**, 14, 3230-3236.
61. Pan, X.; Saddler, J. N., Effect of Replacing Polyol by Organosolv and Kraft Lignin on the Property and Structure of Rigid Polyurethane Foam. *Biotechnol. Biofuels* **2013**, 6, 1-10.
62. Notley, S. M.; Norgren, M., Surface Energy and Wettability of Spin-Coated Thin Films of Lignin Isolated from Wood. *Langmuir* **2010**, 26, 5484-5490.
63. Norgren, M.; Lindstrom, B., Dissociation of Phenolic Groups in Kraft Lignin at Elevated Temperatures *Holzforschung* **2000**, 54, 519-527.
64. Norgren, M.; Edlund, H.; Wagberg, L.; Lindstrom, B.; Annergren, G., Aggregation of Kraft Lignin Derivatives Under Conditions Relevant to the Process, Part I: Phase Behaviour *Colloids and Surfaces A: Physicochem. Eng. Aspects* **2001**, 194, 85-96.
65. Frangville, C.; Rutkevicius, M.; Richter, A. P.; Velev, O. D.; Stoyanov, S. D.; Paunov, V. N., Fabrication of Environmentally Biodegradable Lignin Nanoparticles *ChemPhysChem* **2012**, 13, 4235-4243.

66. Bailey, F. E. J.; Lundberg, R. D.; Callard, R. W., Some Factors Affecting the Molecular Association of Poly(ethylene Oxide) and Poly(acrylic Acid) In Aqueous Solution. *J. Polym. Sci., Part A: Polym. Chem.* **1964**, 2, 845-851.
67. Gundersen, S. A.; Sjoblom, J., High- and Low-molecular-weight Lignosulfonates and Kraft Lignins as Oil/Water-emulsion Stabilizers Studied by Means of Electrical Conductivity *Colloid. Polym. Sci.* **1999**, 277, 462-468.
68. Gundersen, S. A.; Saether, O.; Sjoblom, J., Salt Effects on Lignosulfonate and Kraft Lignin Stabilized O/W-emulsions Studied by Means of Electrical Conductivity and Video-enhanced Microscopy. *Colloids Surf., A* **2001**, 186, 141-153.

Search

[Home](#)[My Springer](#)[Subjects](#)[Services](#)[Publishers](#)[Springer Shop](#)[About us](#)

First Colloid and Polymer Science Lecture awarded to Orlin Velev

Chemical engineer honored for outstanding research in colloid science

New York | Heidelberg, 11 September 2014

The Springer journal *Colloid and Polymer Science* awards Orlin D. Velev from North Carolina State University (USA) the Colloid and Polymer Science Lecture 2014. The award committee chose Velev for his visionary contributions to colloid science and innovative colloidal materials, especially in the areas of particle assembly at interfaces, nanostructures that possess electrical and photonic functionalities, microfluidic devices, and biosensors.

"This is the first time that this award has been presented," said Springer Editor Tobias Wassermann. "Our journal *Colloid and Polymer Science* and the German Colloid Society have established this initiative together with the aim of fostering international scientific exchange in the field of colloid and polymer science."

The *Colloid and Polymer Science Lectures* will be presented at German Colloid Society (Kolloid-Gesellschaft e.V.) meetings. The award committee consists of representatives from the society and from Springer, the editors of the journal, and the respective conference chairs. The *Colloid and Polymer Science Lecture* will be delivered by Velev on 19 September 2014 in Mainz, Germany, at the Colloid Society's 20th Ostwald-Colloquium ("Particles_@_Interfaces").

Velev's lecture will focus on "Magnetically Responsive Pickering Foams, Smart Gels and Dynamic Assemblies." He will also summarize the topic in an invited article in *Colloid and Polymer Science*.

A physical chemist by training, Velev received his PhD from the University of Sofia, Bulgaria, in 1996. He then moved to the University of Delaware in the USA for his postdoctoral studies and began to initiate an innovative program in colloidal assembly and nanomaterials. In 2001 he joined North Carolina State University, where he has held the position of Invista chaired Professor since 2009. Velev has pioneered synthetic strategies for "inverse opals" (a type of three-dimensional photonic crystals), new principles for microscopic biosensors with direct electrical detection, and is active in the fields of electric field assembly and self-assembly processes. He has received numerous prestigious awards for his research and teaching from various organizations.

Colloid and Polymer Science is a leading international journal with a long-standing tradition since 1906 of publishing papers in colloid and polymer science and interdisciplinary interactions. The journal includes original articles, short communications, reviews and perspective articles.

[Further Information](#)[Contact](#)

Share

[Share](#)[Share](#)[Share](#)[Share](#)[Share](#)